AN ABSTRACT OF THE THESIS OF

ELLIOT LEONARD ATLAS for the MASTER OF SCIENCE

in OCEANOGRAPHY presented on January 19, 1973

CHANGES IN CHEMICAL DISTRIBUTIONS AND RELATIONSHIPS DURING AN UPWELLING EVENT OFF THE OREGON COAST

Abstract approved: Redacted for privacy

P. Kilho Park

During cruise Y7006A of the R/V YAQUINA (17-28 June 1970) various stages of upwelling were encountered off the Oregon coast. Eight hydrographic lines between Depoe Bay and Heceta Head were sampled. The Newport hydrographic line was sampled three times during the cruise. Horizontal distributions showed the general features of an upwelling area--low temperature, high salinity, low oxygen and pH, and high nutrients appearing near the coast. Patchiness in the distributions were attributed to local and temporal variations in upwelling combined with biological activity and interaction with the Columbia River.

Temporal changes were assessed using data from the Newport hydrographic line. Relationships between oxygen, temperature, salinity, and nutrients were also investigated. The general conclusions can be summarized as follows:

1. Large changes in chemical distributions can occur within a time scale of several days. The greatest fluctuations were observed within 10 to 15 km of the coast. Changes occurring on a smaller time scale (< 1 day) can also be significant. For cruise Y7006A changes in the chemical distributions resulted primarily from advective transport, biological activity, and interaction with Columbia River water. The roles of mixing and diffusion were not assessed.

2. The velocity structure calculated from the salinity distribution on the Newport line shows a pattern common for upwelling: offshore velocities ranging from 2-18 cm/sec in the surface layers; onshore velocities are in the range of 1-2 cm/sec. The velocity distribution calculated for the 21st to 28th of June suggests a tongue of offshore-moving water sinking below the permanent pycnocline.

3. Transport calculated from the salinity distribution compares well with that computed from wind data. For the 276 hour time interval, both methods show that approximately 8×10^9 g/cm were transported onshore. This corresponds to an onshore transport of nutrients of 1.7, 22, and 38 moles/day/cm of PO_4, NO_3, and SiO_4, respectively.

4. The possibility of large gradients in chemical properties at the surface allows these variables to be quite useful in identification of freshly upwelling waters. This confirms observations by others. Also, because of the different response times of water motion and

biological activity, a combination of biological and hydrographic parameters can be used to identify various stages of upwelling.

5. A comparison of PO_4 concentrations on surfaces of constant sigma-t indicated a nutrient source low in the water column of the inshore stations. Remineralization of organic detritus in the shelf sediments is likely a large contributor to this source.

6. The flux of oxygen is from the atmosphere to the sea in water which has recently upwelled. This is expected because the water arriving at the surface is undersaturated with respect to atmospheric oxygen. This effect is also reflected in the preformed nutrient values. Biological activity will also increase the oxygen content of the surface waters.

7. The combination of NO_3: PO_4 and SiO_4: PO_4 ratios can indicate, to some extent, the origin and "photosynthetic age" of upwelled water. These ratios also indicate an abundance of phosphate relative to silicate and nitrate (compared to normal assimilation ratios).

8. Temperature inversions were found to coincide with oxygen inversions at inshore stations after upwelling had continued for approximately 12 days. These inversions suggest recent contact with the atmosphere and tend to support the conceptual model of upwelling presented by Mooers et al. (1972). That not all temperature inversions contained oxygen inversions can be explained by in situ oxidation of detritus both entrained in and falling through the water mass, and by mixing and diffusion.

Changes in Chemical Distributions and Relationships during an Upwelling Event off the Oregon Coast

by

Elliot Leonard Atlas

A THESIS

submitted to

Oregon State University

in partial fulfillment of
the requirements for the
degree of

Master of Science

June 1973

APPROVED:

Redacted for privacy

Professor of Oceanography in charge of major

Redacted for privacy

Dean of School of Oceanography

Redacted for privacy

Dean of Graduate School

Thesis presented January 19, 1973

Typed by Suelynn Williams for Elliot Leonard Atlas

ACKNOWLEDGMENTS

I would like to express thanks to the many people who helped in the preparation of this thesis: to Kilho Park, for serving as major professor; to Louis Gordon, for the time he devoted to helpful discussions and criticisms of this work, and for his patience; to Robert Smith, for his aid in helping me with the physical aspects of upwelling, and for his criticisms of this manuscript; to Kent Kantz and Saul Alvarez-Borrego, for their helpful comments; to Suelynn Williams, for working miracles in the preparation and typing of this thesis; to Richard Tomlinson, Dave Standley, Lynn Jones and Joyce Shane, for aid in data reduction and the drafting of figures; to John Callaway, for performing many of the nutrient analyses; and to the officers, crew, and scientific party of cruise Y7006A, for their hard and diligent work. The love and encouragement given me by my wife, Holly, was invaluable.

This thesis was supported under NSF grant GA 12113 and ONR contract N00014-67-A-0369-0007 under project NR 083-102.

TABLE OF CONTENTS

LIST OF TABLES

LIST OF FIGURES

LIST OF FIGURES CONTINUED

LIST OF FIGURES CONTINUED

CHANGES IN CHEMICAL DISTRIBUTIONS AND RELATIONSHIPS DURING AN UPWELLING EVENT OFF THE OREGON COAST

CHAPTER ONE

INTRODUCTION

Upwelling occurs along the western margin of continents in the Northern Hemisphere when wind blowing from the north causes a transport of water away from the coast; this water is then replaced near the coast by deeper water. Smith (1968) defines upwelling as "an ascending motion, of some minimum duration and extent, by which water from subsurface layers is brought to the surface layer and is removed from the area by horizontal flow." Off the Oregon coast, this horizontal transport is induced by strong northerly winds. These northerlies predominate in the summer months under the influence of the North Pacific High, but variations in these winds can cause upwelling to subside (Kantz, 1973) or to vary in strength (Smith, 1968).

Smith reviews the theoretical framework for upwelling and discusses some of the general effects of upwelling. Pillsbury (1972) summarizes hydrographic data on the Newport and Depoe Bay hydro-

graphic lines off the Oregon coast. His data include a ten-year record (1960-1970) of observations taken during the months April-September. These months are generally taken to be the "upwelling season" off Oregon. His work presents the average characteristics of upwelling off Oregon. He notes that though the long range seasonal pattern of upwelling is quite smooth, short-term variations are quite important. Pillsbury's work also presents a literature review on the physical oceanographic studies pertaining to upwelling off the Oregon coast. This review is complete through 1971. An intensive study of the Oregon upwelling regime is currently in progress (CUE, 1972) but, as of this writing, only preliminary results have been released.

Chemical features of upwelling off the Oregon coast have also been under close scrutiny. Park et al. (1962) noted that high values of alkalinity, phosphate, and salinity and low values of dissolved oxygen and pH appeared inshore during Oregon's coastal upwelling. They suggested the use of pH as a useful indicator of upwelling, because of its ease of measurement. Stefánsson and Richards (1963, 1964) discussed the distribution of dissolved oxygen, nutrients, and density off the Oregon and Washington coasts. They concentrated on the effect of the Columbia River on these distributions, but noted the effect of upwelling in altering distributions along the coast. Their 1964 paper suggested that the subsurface maximum in dissolved oxygen commonly observed off the Oregon and Washington coast during the summer is

produced by downward, offshore advection of aerated, upwelled water. Park (1968) discussed the seasonal pattern of alkalinity and pH off the coast of Oregon, and noted how upwelling affects these distributions. Upwelling was also regarded as a major factor in changing chemical distributions by Ball (1970) in his study of seasonal distribution of nutrients off the Oregon coast. Hager (1969) showed that upwelled water is a major factor in the offshore distribution of silicate. Kantz (1973) analyzed chemical data, including the partial pressure of CO_2 (P_{CO_2}), for two cruises in March and June, 1971. Contrary to the general seasonal trend associated with upwelling, he found indications of upwelling during March, and a deteriorated upwelling regime during June. Gordon (1973) concentrated on P_{CO_2} in his discussion of upwelling off Oregon. He described seasonal fluctuations in the distribution of P_{CO_2} and noted that variations occurring on the time scale of 2-5 days can be of the same magnitude as the seasonal changes.

The picture of upwelling over long (seasonal) cycles is fairly well established. Not enough data has been collected to begin to discuss longer (> one year) cycles. As was noted by Pillsbury (1972) and Gordon (1973), short-time scale variability is significant in the Oregon upwelling regime. Work by Jones (1972) off the coast of Africa indicates that this short-time scale variability is not unique to the Oregon coast.

The data collected during June, 1970 off the coast of Oregon presented a unique opportunity to examine upwelling and its variability on the order of 3-12 days. The winds prior to and during the beginning of the cruise were rather light and variable. They then shifted to strong northerlies for about seven days, and once again became variable at the end of the cruise. Two hydrographic lines were sampled three times each: prior to, during, and following the period of strong northerlies. A rather complete set of both hydrographic and chemical data was obtained. Included in this work are discussions of temperature, salinity, density, dissolved oxygen, phosphate, nitrate, silicate, and pH. Horizontal distributions and a time series of vertical distributions on the Newport hydrographic line are given.

CHAPTER TWO

METHODS AND OBSERVATIONS

Water samples were collected from NIO (National Institute of Oceanography) bottles for determination of salinity, dissolved oxygen, pH, alkalinity, total CO_2, nitrate + nitrite, silicate, and phosphate. Temperature was measured with reversing thermometers. All analyses, except for nutrient analyses, were performed at sea.

Salinity was measured with an inductive salinometer (Hytech, Model 6220) according to the method described by Brown and Hamon (1961). Dissolved oxygen was measured using the modified Winkler method given in Strickland and Parsons (1968). Dissolved oxygen concentrations will be referred to simply as oxygen. An Orion Model 801 digital pH meter was used for pH and alkalinity measurements. The alkalinity was determined on previously measured pH samples using the method of Anderson and Robinson (1946). Total CO_2 was determined by a gas chromatographic technique (Park, 1965). Further description of the methods can be found in Wyatt et al. (1971).

Nutrient concentrations were determined using an AutoAnalyzer® following the methods outlined in Atlas et al. (1971). Throughout this work, the following terminology will be used: reactive phosphate

(Strickland and Parsons, 1968) will be called phosphate; reactive silicate will be called silicate; and the measured quantity of nitrate + nitrite will be called simply nitrate. Unless otherwise noted, nutrient concentrations will be given in μM (μg-at/l).

Nutrient samples were frozen for periods ranging from six months to one year. If the water is analyzed immediately after thawing, silicate concentrations > 50 μM will show a lower concentration compared to non-frozen samples (Hager, 1969). No such systematic effect is seen for the other nutrients (Stefánsson and Richards, 1963). Since most silicate values were less than 50 μM the data were not corrected for this effect.

All silicate data were corrected for standard impurity and non-linearity according to:

$$Si_{corr} = 0.975\ (0.675 + 0.916 \times Si_{meas} + 0.0026 \times Si^2_{meas}) \quad (1)$$

where: Si_{corr} = the corrected SiO_4 concentration (μM)

Si_{meas} = the measured SiO_4 concentration (μM)

The nonlinearity (deviation from Beer's Law) was introduced by analyzing the silicate with white light, rather than filtered light (Kolthoff et al., 1969). Laboratory experiments to compare the results of using white versus filtered light were made, and a polynomial describing observed versus true concentrations was fitted to the data by the method of least squares. The factor 0.975 is used to correct for

standard impurity. Sodium silicofluoride (Na_2SiF_6), which is used as the silicate standard, was compared against 99.999% SiO_2 fused with Na_2CO_3. The Na_2SiF_6 used for these analyses was found to be 97.5 ± 0.5% pure, compared to the 99.999% SiO_2.

During most periods of daylight on the cruise secchi disk readings were taken. These readings were used to determine the depth of the euphotic zone (Poole and Atkins, 1929 as cited in Sverdrup et al., 1942).

All regression analyses were calculated with a CDC 3300 digital computer using the program *SIPS (OSU, Department of Statistics, 1971).

Cruise Y7006A of the R/V YAQUINA began on 17 June and ended 29 June 1970. That part of the cruise discussed in this study consists of eight hydrographic lines extending 45 km from the coast bounded by Heceta Head on the south and Depoe Bay on the north. Figure 1 shows the stations occupied. The Newport line and the Depoe Bay line were occupied three times each during the cruise.

Throughout this work, initials will be used to designate each hydrographic line. Numbers following the initials are station designations which correspond to the distance from the coast in nautical miles. Table 1 gives the times for each of the hydrographic lines.

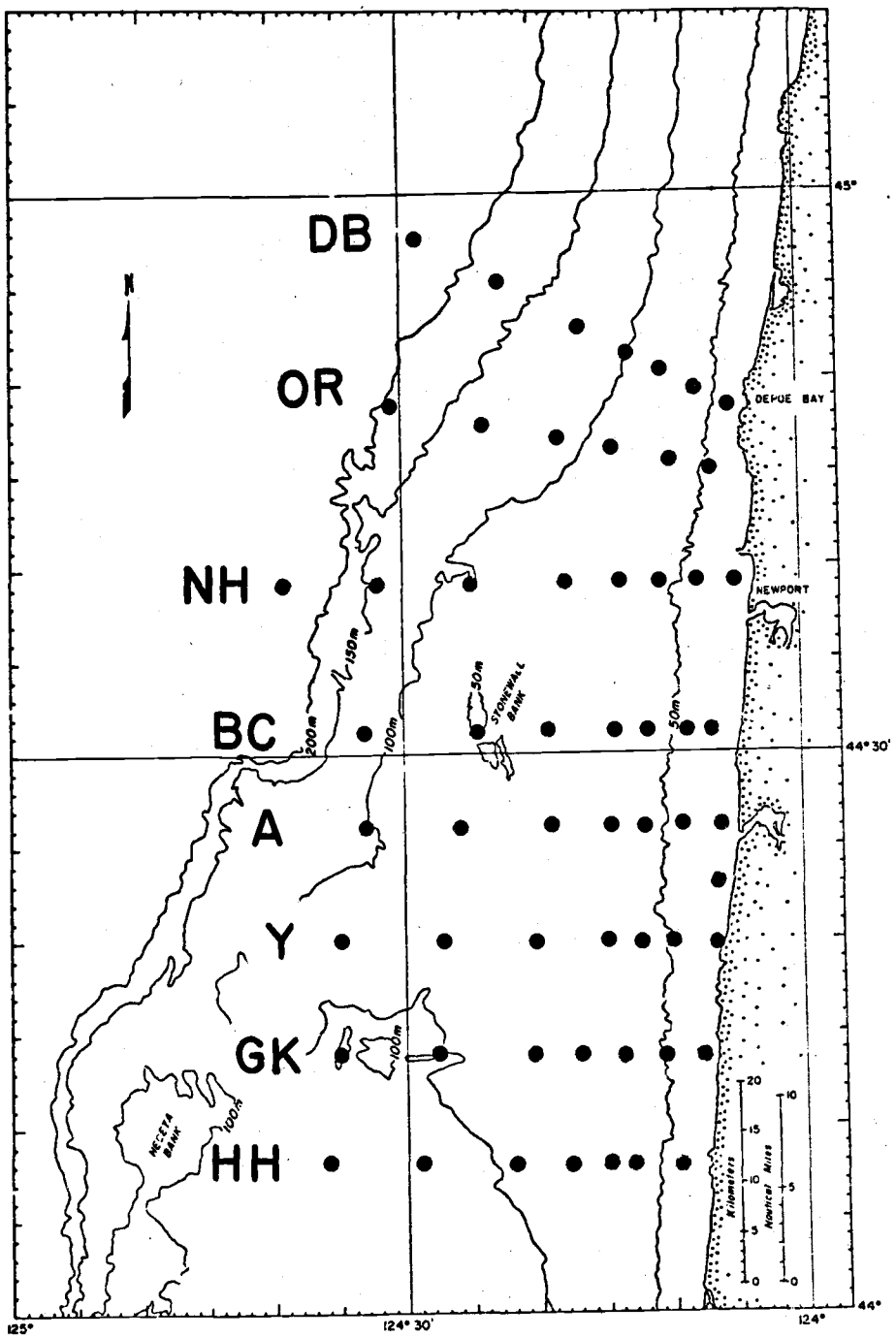

Figure 1. Station locations for cruise Y7006A.

Table 1. Times of occupation for each hydrographic line sampled during cruise Y7006A.

Line	Abbr.	Begin Line	Local Time	End Line	Local Time	Date
Depoe Bay	DB	1DB-1	1310	1DB-25	0315	16-17 June
		2DB-20	0030	2DB-1	1103	22 June
		3DB-25	0300	3DB-10	0900	27 June
Otter Rock	OR	OR-2	0955	OR-20	2135	21 June
Newport	NH	1NH-25	0840	1NH-1	2214	17 June
		2NH-25	2010	2NH-1	0740	20-21 June
		3NH-1	0710	3NH-25	2035	28 June
Beaver Creek	BC	BC-2	0800	BC-20	1745	20 June
Alsea	A	A-20	1940	A-1	0630	19-20 June
Yachats	Y	Y-1	0520	Y-20	1750	19 June
Gwynn Knoll	GK	GK-20	1545	GK-1	0250	18-19 June
Heceta Head	HH	HH-1	0330	HH-20	1345	18 June

For lines run more than once a numeral will precede the initials to indicate its place in the series (e.g., 2NH-15 = 15 mile station, second running of NH line). A table of conversions from nautical miles to kilometers is given below.

Table 2. Conversion of nautical miles to kilometers.

Nautical miles	1	2	3	4	5	7	10	15	20	25
Kilometers	1.9	3.8	5.6	7.4	9.3	13.0	18.5	27.8	37.0	46.3

The data used in this study are compiled in Wyatt et al. (1971, 1972).

CHAPTER THREE

DISTRIBUTIONS OF VARIABLES

Horizontal Distributions

This section will review the distribution of chemical and physical properties at the sea surface during cruise Y7006A. The area between the Heceta Head and Depoe Bay hydrographic lines was densely sampled (Figure 1) with much emphasis placed on the inshore 20 km. This was a fortunate sampling plan, as most of the interesting features noted occurred inshore of 20 km. The sequence covered in this section begins at the HH line and ends at the DB line. This includes the second occupations of the NH and DB lines.

The locations and magnitudes of the maximum and minimum values encountered during this cruise are listed in the results section following the name of each variable. This is done to give a better indication of the range of each variable than can be obtained from the surface maps.

Results

Temperature (Figure 2). (T_{min} 7.39°C at 2DB-1; T_{max} 13.12°C at

GK-20).

The water temperature between the HH and Y lines is fairly warm and constant, generally falling into the range 11-13°C. Of the three lines, HH, GK, and Y, the Y line shows the coolest inshore temperature of 9.08°C at Y-1. Generally, the coolest temperatures are found nearest the coast, though there is not a strict trend of increasing temperature with increasing distance from shore. Relative minima are found at HH-15-20, GK-10, and Y-10 and Y-20. The A line shows a maximum of 12.13° at A-20. Inshore water becomes progressively cooler north of the A line. Between the A and BC lines the 10° and 11° isotherms move offshore approximately 9 and 14 km, respectively, although the 9° isotherm remains roughly constant at 6 km offshore. At the DB line (the furthest north) the 9° isotherm has progressed to ~15 km offshore. Water of < 8°C has appeared at OR-1 and is also found at DB-1 and DB-3. A patch of water > 10°C is found around NH-7 and NH-10. Between the NH line and the DB line isotherms of 10°C and 11°C have moved inshore ~10 km each, thus opposing the offshore movement of cooler isotherms. The inshore trend of warmer isotherms roughly parallels the bottom contours in the area.

Salinity (Figure 2). (S_{min} 31.68‰ at NH-25; S_{max} 33.83‰ at 2DB-1).

In all cases, except NH-10, there is a salinity decrease with increasing distance from shore, although the rate of decrease varies

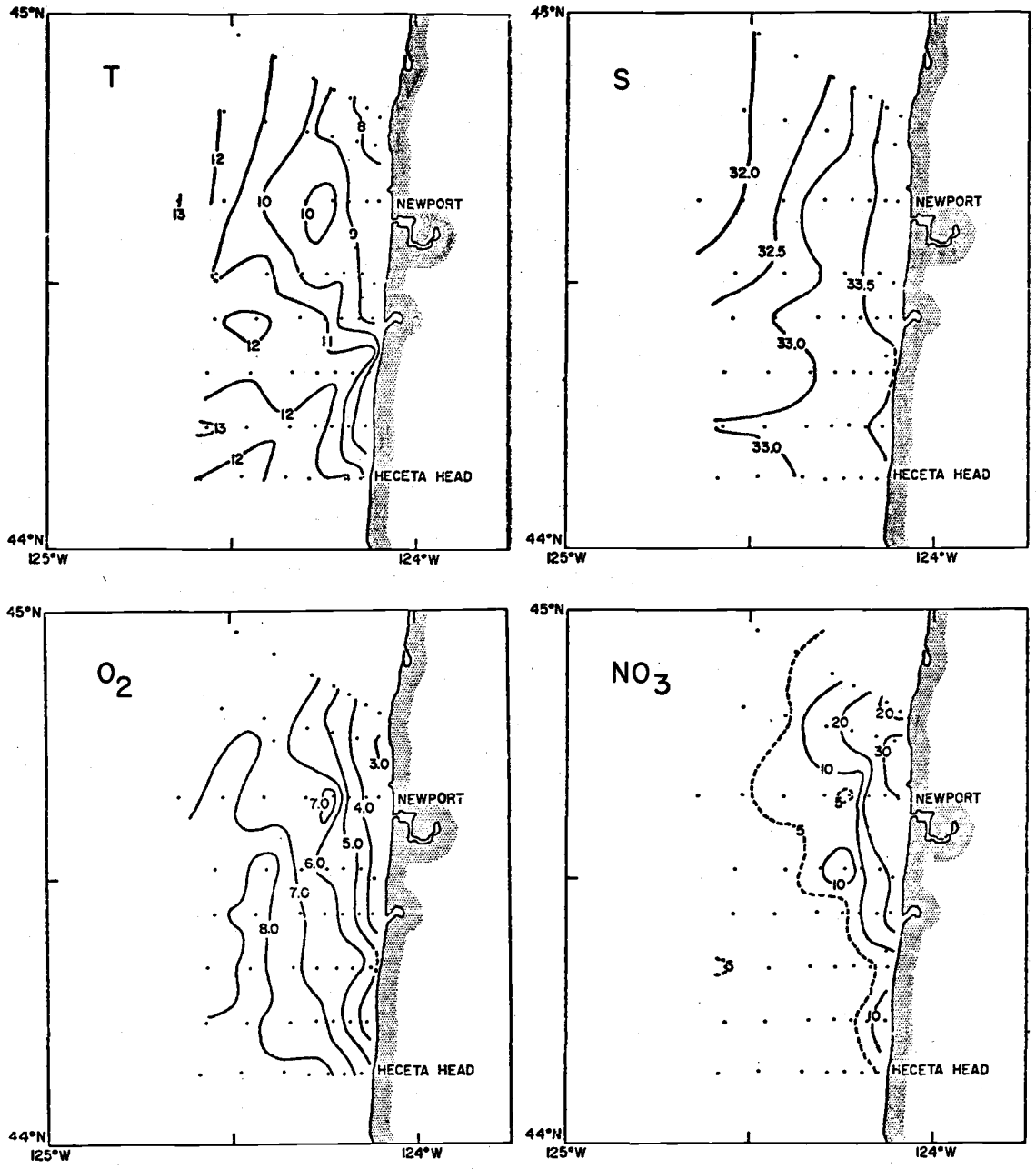

Figure 2. Surface distribution of temperature (°C), salinity (‰), oxygen (ml/l), and NO_3 (μM). (The 5 μM NO_3 contour is dotted because it is a different contour interval from the remainder of the isograms.)

from line to line. The GK line shows a slightly greater salinity than the adjacent hydrographic lines; at the nearest inshore station on the GK line (GK-1) the salinity is about 0.15‰ higher than either HH-1 or Y-1. Further north, movement of salinity isograms away from the coast is not nearly so pronounced as that seen in the temperature distribution. As in the temperature distribution, the salinity isograms north of the A line seem to roughly parallel the bottom contours. The three inshore stations (NH-1, OR-1, DB-1) show practically the same salinity, ~ 33.82 (± 0.01)‰, the highest measured at the surface.

Sigma-t (Figure 3). (sigma-t_{min} 23.85 at 2NH-25; sigma-t_{max} 26.48 at 2DB-1).

The sigma-t distribution closely resembles the salinity distribution. In all cases, again with the exception of NH-10, sigma-t values decrease with increasing distance from shore. North of the A line at the one-mile stations, sigma-t values are found to be progressively higher, reaching a maximum of 26.48 at DB-1. A small patch of water > 26.0 sigma-t is seen at the one-mile station on the GK line.

Nitrate (Figure 2). ($NO_{3_{min}}$ 0 at several places; $NO_{3_{max}}$ 33.4 μM at OR-2).

The surface NO_3 distribution shows striking variations which range from ~ 0 to > 30 μM NO_3. The three most southerly lines (HH, GK and Y) show their highest NO_3 concentrations at the nearest

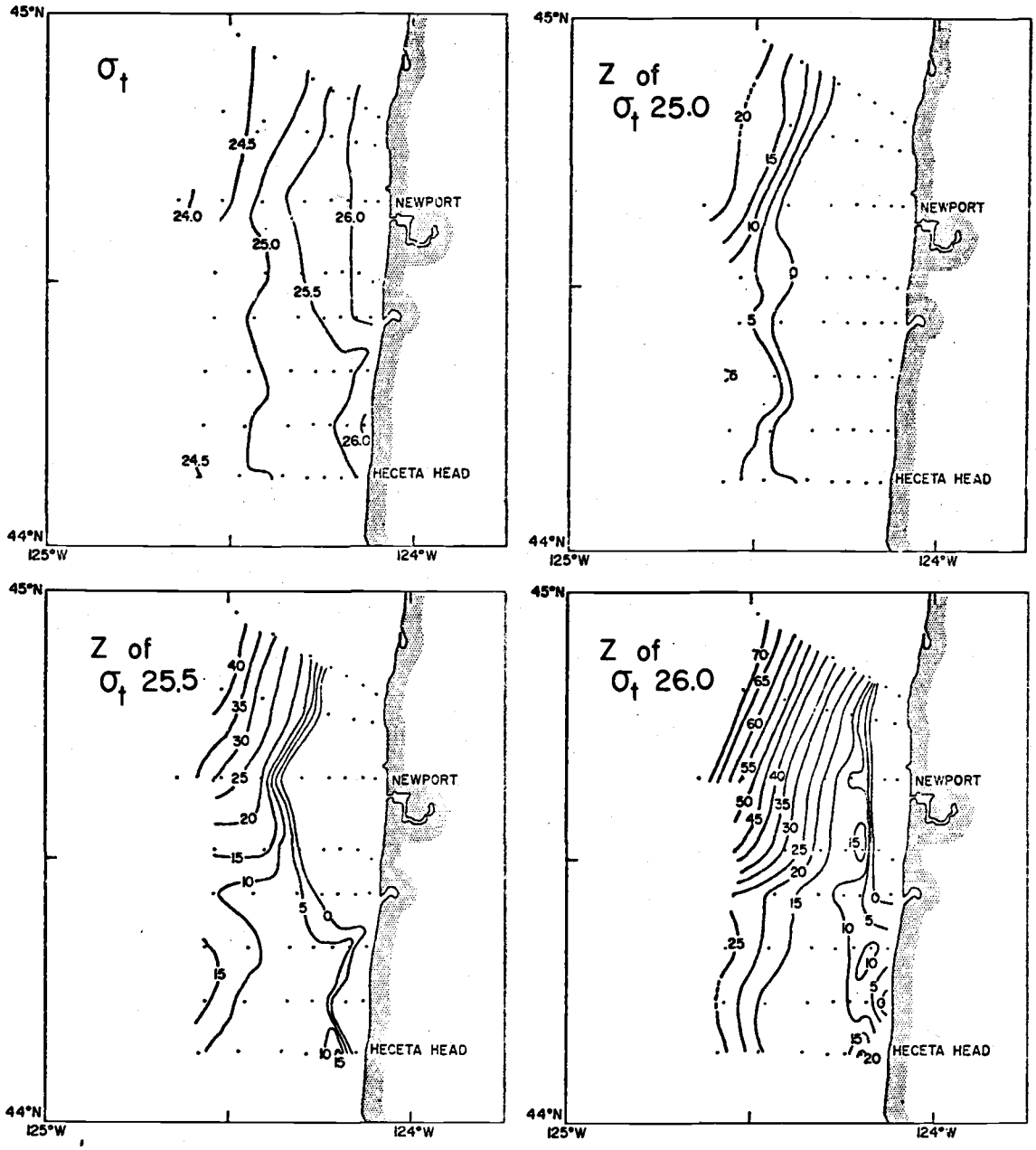

Figure 3. Surface distribution of sigma-t and depths of 25.0, 25.5, and 26.0 sigma-t surfaces in meters.

inshore station, with GK-1 showing an anomalously high NO_3 value of 17.6 μM (compared to adjacent-line values of 4.6 and 8.8 μM). Along the Y line are patches of water with NO_3 concentration close to 5 μM surrounded by water nearly depleted of NO_3. The 5 μM NO_3 contour progresses offshore in an apparently stepwise fashion from the Y line to tne NH line. This offshore progression reverses at the NH line. Both the BC and NH lines have patches of water low in nitrate at ~ 12 km from shore. In contrast to salinity and temperature, which show extrema at DB-1, NO_3 concentrations are maximum at OR-2.

Oxygen (Figure 2). ($O_{2_{min}}$ 2.88 ml/l at OR-2; $O_{2_{max}}$ 8.74 ml/l at HH-20).

Oxygen shows a pattern inverse to that of the nitrate distribution. Lowest values tend to be found nearest the coastline, with higher values offshore. Contours below 5 ml/l O_2 tend to parallel the coast, with occasional low values (~ 3 ml/l) appearing at some of the nearest inshore stations. Relative maxima in oxygen are located along a band approximately 27 km offshore between the GK and BC lines (not contoured), and also at NH-7. The water is undersaturated with respect to atmospheric oxygen continuously along the coast inshore of an approximate diagonal from HH-1 to ~ 20 km offshore along the DB line. The 100% saturation contour corresponds roughly to the 6 ml/l O_2 contour. The extrema in percent saturation are found at

the same places as the extrema in dissolved O_2. The range is from 43% to 142% of saturation with respect to atmospheric O_2.

Phosphate (Figure 4). ($PO_{4_{min}} \sim 0.1$ μM at various places along HH and GK lines; $PO_{4_{max}}$ 2.67 μM at NH-1).

The phosphate distribution closely resembles the distribution of nitrate in the surface waters, except that where there was essentially no NO_3 (< 0.1 μM) phosphate is present in quantities ranging from 0.07 to 0.3 μM PO_4. As found in the NO_3 distribution, inshore PO_4 concentrations are always higher than those found offshore, although patches and bands of relatively low PO_4 water are found throughout the area. The 1 μM PO_4 contour approximates water of 100% O_2 saturation. A patch of water anomalously high in PO_4 (compared to adjacent stations) is found at GK-1.

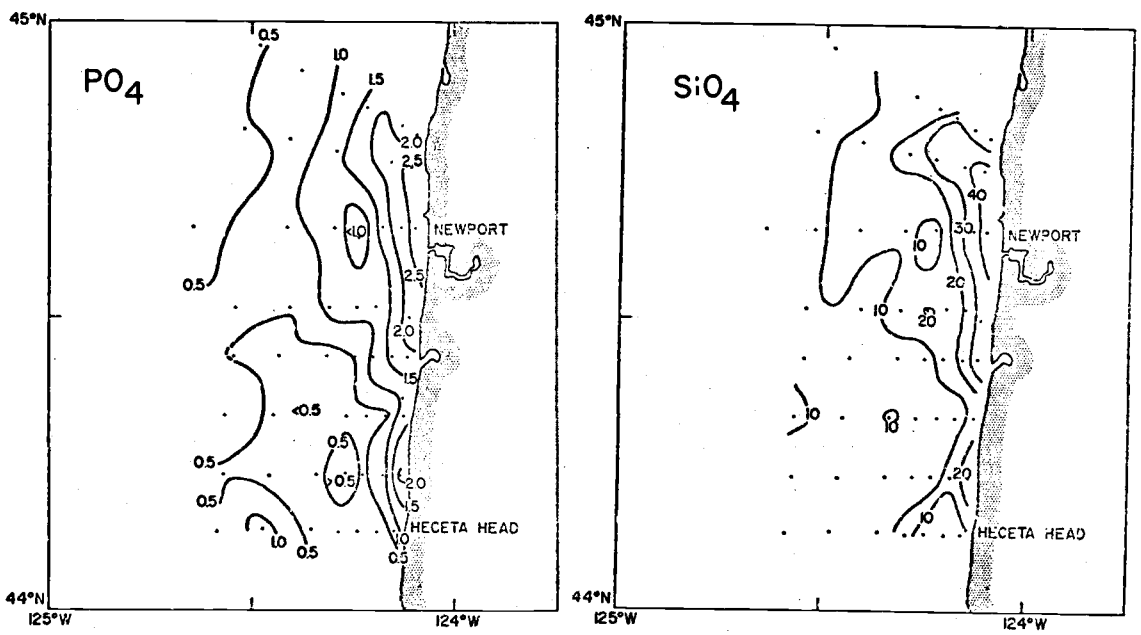

Figure 4. Surface distribution of phosphate (μM) and silicate (μM).

Silicate (Figure 4). $SiO_{4_{min}}$ ~ 2 μM in southern section and offshore; $SiO_{4_{max}}$ 48 μM at OR-1).

The silicate distribution closely follows the pattern seen in the other two nutrients. The main features are essentially the same --high nutrients measured inshore and lower nutrient water found progressively further offshore as one moves north. Anomalous patches (i.e. deviations from strict banding) seen in the silicate distribution also correspond to the ones noted in the other nutrient distributions.

Depth of sigma-t surfaces (Figure 3).

The sigma-t surfaces chosen are 25.0, 25.5, and 26.0. They roughly approximate the base of the seasonal pycnocline, the upper region of the permanent pycnocline, and the lower region of the permanent pycnocline, respectively (Collins, 1964).

Sigma-t 25.0--The 25.0 sigma-t contour at zero depth runs roughly parallel to the coastline about 20 to 28 km offshore. South of the BC line, the topography of the sigma-t 25.0 surface is relatively flat. A slight uplifting of this surface is seen at Y-20. Otherwise this sigma-t surface is found progressively deeper offshore. On the NH line and further north, the 25.0 sigma-t surface sinks deeper, and with a slightly larger gradient (~ 1 m/2 km), than further south. The maximum depth reached is 24.5 m at NH-25. Of the stations 20 miles offshore, the greatest depth of this sigma-t surface is observed at DB-20.

Sigma-t 25.5--The zero depth contour of the 25.5 sigma-t surface shows an offshore trend between the Y and NH lines, going from ~ 12 km to 20 km offshore. North of the NH line, the zero depth contour moves inshore about 6 km, following the trend of the bottom contours. As with the 25.0 sigma-t surface, the southern section of the 25.5 sigma-t surface shows a relatively flat topography. The steepest gradients are north of the BC line. Following a gradient of ~ 8 m/km between 0 and 15 m, the gradient lessens and stabilizes at ~ 3 m/km. The maximum depth reached within the 20 mile stations is 44 m at DB-20.

Sigma-t 26.0--Water having a value of 26.0 sigma-t units appears at the surface near A-3 and continues northward roughly parallel to the coastline. A small patch of 26.0 sigma-t water also surfaces inshore of GK-3. Similar to the other sigma-t surfaces described, a generally flat topography of the 26.0 sigma-t surface is found south of the A line. A small uplift of the 26.0 sigma-t surface at ~ 12 m extends north from the A-line ~ 20 km offshore and disappears north of the NH line. Again, the maximum gradient is between 0 and 15 m at stations north of the BC line. The contours > 10 m run in a generally NNW direction, similar to the bottom contours.

Discussion

The horizontal distributions of the parameters presented above may be viewed as a superposition of a spatial distribution on a temporal distribution. The wind pattern during the cruise showed winds consistently blowing from the north, the average northerly component of the wind increasing from ~ 8 knots prior to the start of the HH-line to ~ 18 knots at the end of the DB-line (Figure 5). Prior to the cruise, winds were variable, having northerly components ranging from approximately +10 to - 10 knots. There was however, a 3-4 day stretch of moderate northerly winds. These few days may have been enough to induce a modest upwelling along the coast. Possibly the one day of 10-knot southerly winds and the several days of light northerly winds (prior to the cruise) would have been sufficient to inhibit the upwelling which had been in progress earlier. At the HH line, waters of sigma-t 25.5 are seen at the surface. This value of sigma-t is always found in the upper part of the permanent pycnocline (Collins, 1964), and thus would seem to indicate some moderate upwelling before the cruise.

The patch of cold, nutrient-rich water seen near the coast on the GK line may be interpreted in two ways. First, it could indicate the first noticeable effects of renewed upwelling. As such, it would indicate a response time for upwelling on the order of two days.

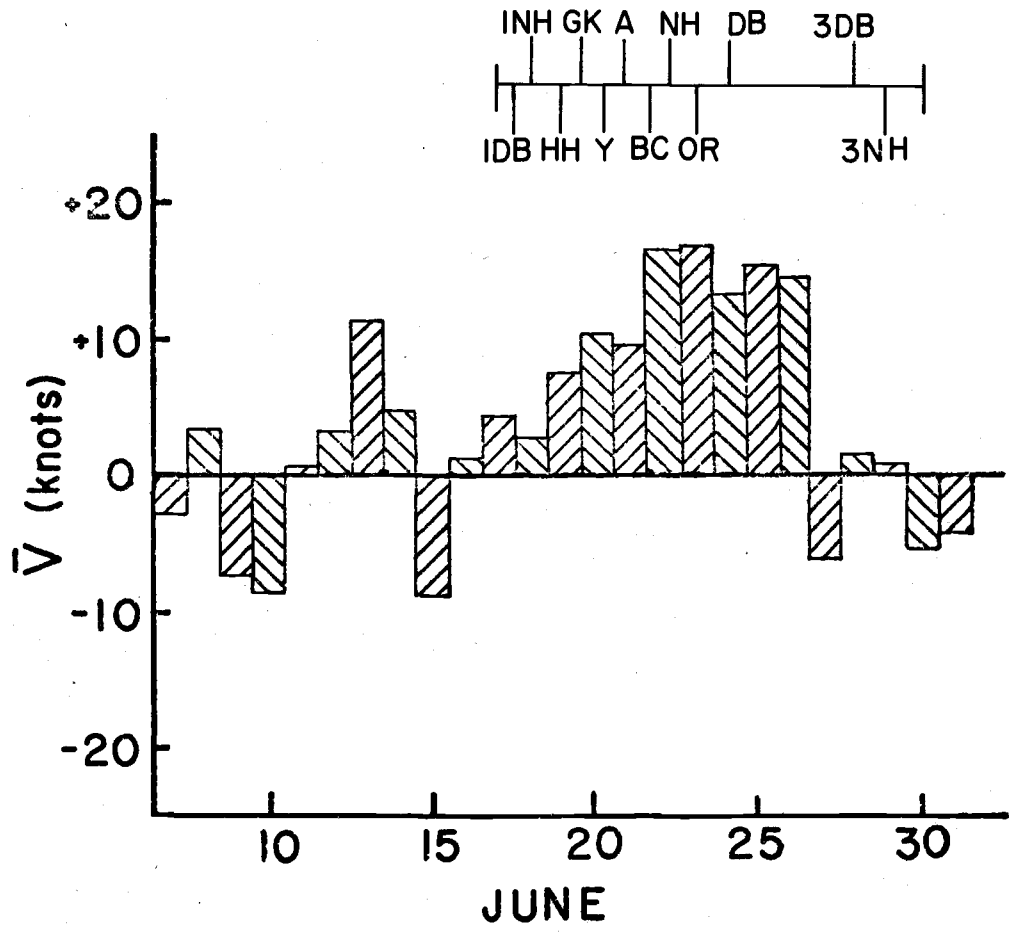

Figure 5. Daily averages of the northerly component of wind velocity measured at the south jetty, Newport, Oregon. ($\bar{V}$ is positive when the wind is blowing from the north.)

Alternately, this patch may be a remnant of a strong, localized upwelling, which was not destroyed so completely as the upwelling in the surrounding areas. There is no compelling reason to favor either of these alternatives. Because of the great variability and the rapid changes in the coastal regime, synoptic measurements of chemical variables are virtually impossible to obtain. Thus, separation of local versus time changes of variables in the upwelling area is only speculative.

Further north along the coast, it seems likely that the general offshore movement of isograms indicates more of a time change than a spatial difference. (See discussion of changes on the NH line, p. 38-42). The tendency for isograms to shift inshore north of the NH line might possibly be due to the presence of Columbia River water offshore. Also, the surface frontal zone is found to "focus" on cape areas along the coast (Arthur, 1965). In this case, the trend of the isograms is toward Cascade Head, about 30 km north of Depoe Bay.

Anomalous features appear in the surface distribution. One such feature is the pool of relatively warm water around NH-7. A similar, but not so pronounced, feature seen at BC-5 might be a southward extension of this pool of water. Other characteristics of this water are relatively lower nutrients, lower salinity, and higher oxygen than the surrounding waters. It is typical of "older" surface water, as opposed to freshly upwelled water. Possibly this water was

advected in from further north and persisted in a generally southerly direction, intersecting the newly upwelled water. Alternately, a secondary upwelling offshore of NH-7 would produce the observed distribution.

The relationship between temperature and oxygen (and nutrients) seen at the nearshore stations on the OR and DB lines is slightly different from that which might be expected. One would expect the coldest surface water to be the lowest in oxygen and the highest in nutrients. The water's cool temperature would indicate its recent arrival at the surface; it wouldn't have had time to be heated and/or mixed with warmer adjacent waters. It would seem, too, that this water would not have been at the surface long enough for initiation of photosynthesis or oxygen exchange. However, the slightly warmer water at OR-1 has lower oxygen and higher nutrient concentrations than at DB-1. Discarding the possibility of bad data (oxygen, nutrients and temperature are measured independently), a reasonable suggestion is that the water at DB-1 contained an oxygen maximum (nutrient minimum) before arrival at the surface.

Further discussion of changes in the surface properties will be presented in the section dealing with the vertical distributions on the Newport line (see p. 38-42).

The areal distribution presented above clearly indicates the dynamic nature of the coastal upwelling system. The simplest con-

ception of upwelling would be a model having water moving onshore from some depth, arriving at the nearshore surface and then being transported offshore at the surface. Given uniform water velocities along the coast this would produce a surface distribution pattern showing north-south bands of a variable grading from values characteristic of the source waters to values found on the surface further offshore. Adding localized phytoplankton blooms would produce areas of high oxygen and low nutrients as deviations from the banding still seen in the physical parameters. The Columbia River plume, driven south by the prevailing winds, would add more variability and a more intense density gradient perpendicular or diagonal to the coast. Now the banding, still a general feature, would show bends and deformations, depending on the influence of the river water. Surface current variability would differentially move parcels of water around the area, pushing plume water into newly upwelled water. Finally, adding the time and space variations of upwelling along the coast, one would arrive with the distributions presented above.

In summary, the surface distribution seems to be dominated by the hydrographic trends associated with upwelling (inshore cold, saline surface water, high nutrient concentrations, low oxygen concentrations) although patchiness occurs in these physical and chemical variables. This patchiness can be the result of local biological activity, surface currents, and interaction with Columbia River water,

although the relative contributions of each of these is difficult to isolate.

Vertical Distributions on the Newport Hydrographic Line

Large changes in chemical distributions were observed to occur during the successive occupations of the Newport hydrographic line. This section will focus on these temporal variations as evidenced in the vertical sections.

The Newport hydrographic line was sampled three times during cruise Y7006A. As mentioned before, a numeral will precede "NH" to indicate its order in the sequence. Numbers following "NH" will be station designations. These latter numbers also indicate distance from the coast in nautical miles. Thus, 2NH-15 will indicate the 15-mile station the second time the Newport line was run. The times and dates for 1NH-3NH are:

	Date (1970)	Local Time
1NH	June 17	0840-2214
2NH	June 20-21	2010-0740
3NH	June 28	0710-2035

The stations occupied were NH-1, -3, -5, -7, -10, -15, -20, and -25. Sampling locations are indicated in Figure 6.

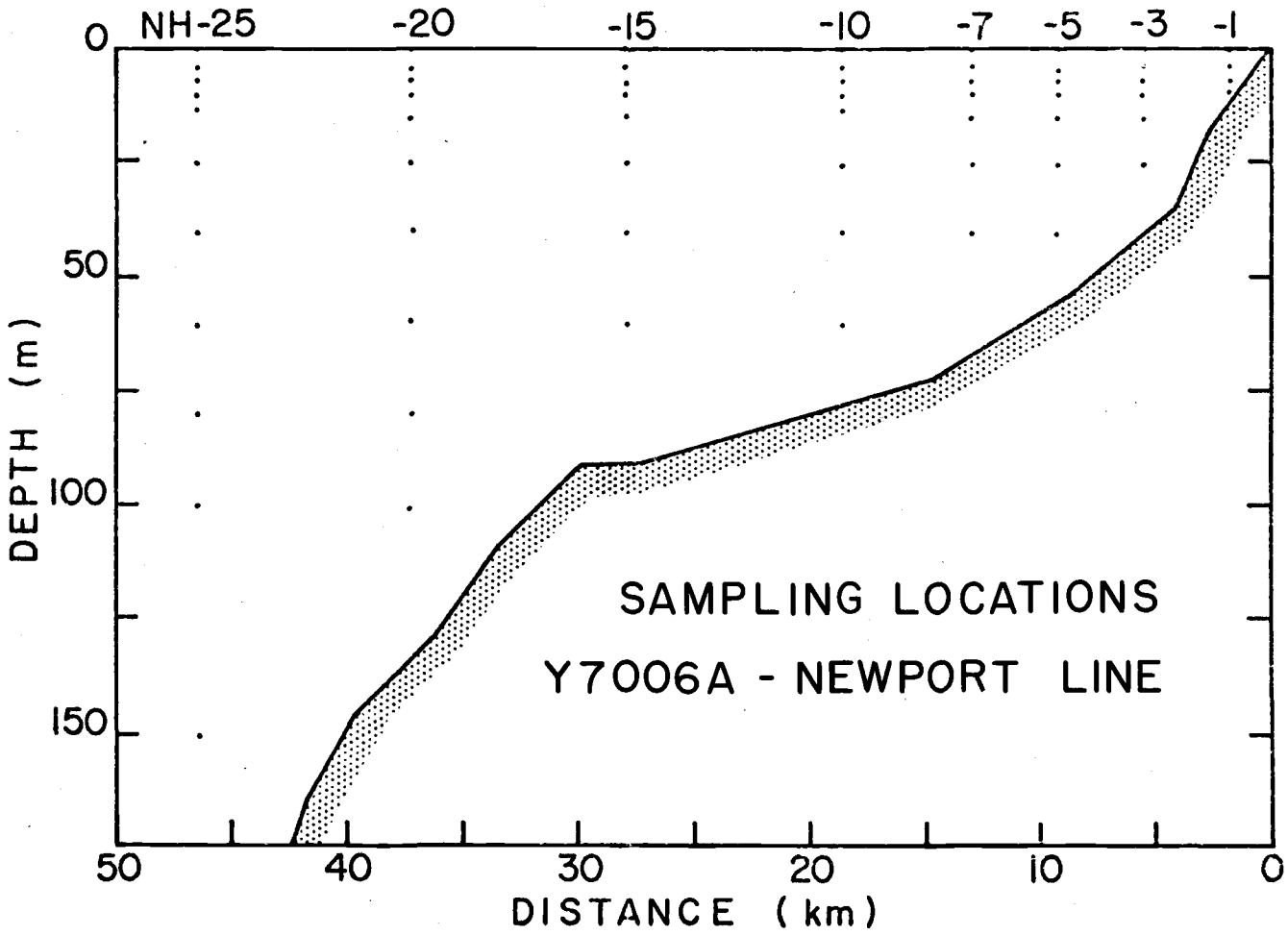

Figure 6. Sampling locations on the Newport hydrographic line--Y7006A.

Results

Temperature (Figure 7). The isotherms during 1NH were essentially horizontal. Isotherms of $\geq$13° C to 8° C are roughly parallel to the sea surface, while the 7° C isotherm follows the bottom but intersects it near 1NH-3. Surface layer and inshore changes are quite abrupt between 1NH and 2NH. Note that the 12° C isotherm on 2NH, found four days earlier at ~ 10 km offshore, has moved to roughly 40 km offshore. Surface temperatures inshore have dropped about 3° C. Isotherms $\geq$ 10° C become slightly shallower offshore of 2NH-5 compared to 1NH. A temperature inversion not seen during 1NH is seen at 2NH-25; it is likely to have been advected into the region from further north. (A similar inversion was seen during the 1DB line, but none were noticed south of the NH line.) All traces of water > 11° C have been removed inshore of 25 miles by the time of 3NH. A newly formed temperature inversion (not contoured) is found inshore around NH-5-7. This will be discussed more fully later (see section on O_2-T-S, p. 82-92). The older temperature inversion seen at 2NH-25 has disappeared from the 3NH section. Further, the 7° C isotherm has risen at 3NH-25 by about 40 m, indicating intrusion of deeper water.

Salinity (Figure 8). Columbia River influence is felt as far inshore as 1NH-7, as indicated by salinities < 32-32.5‰ (Cissell, 1969).

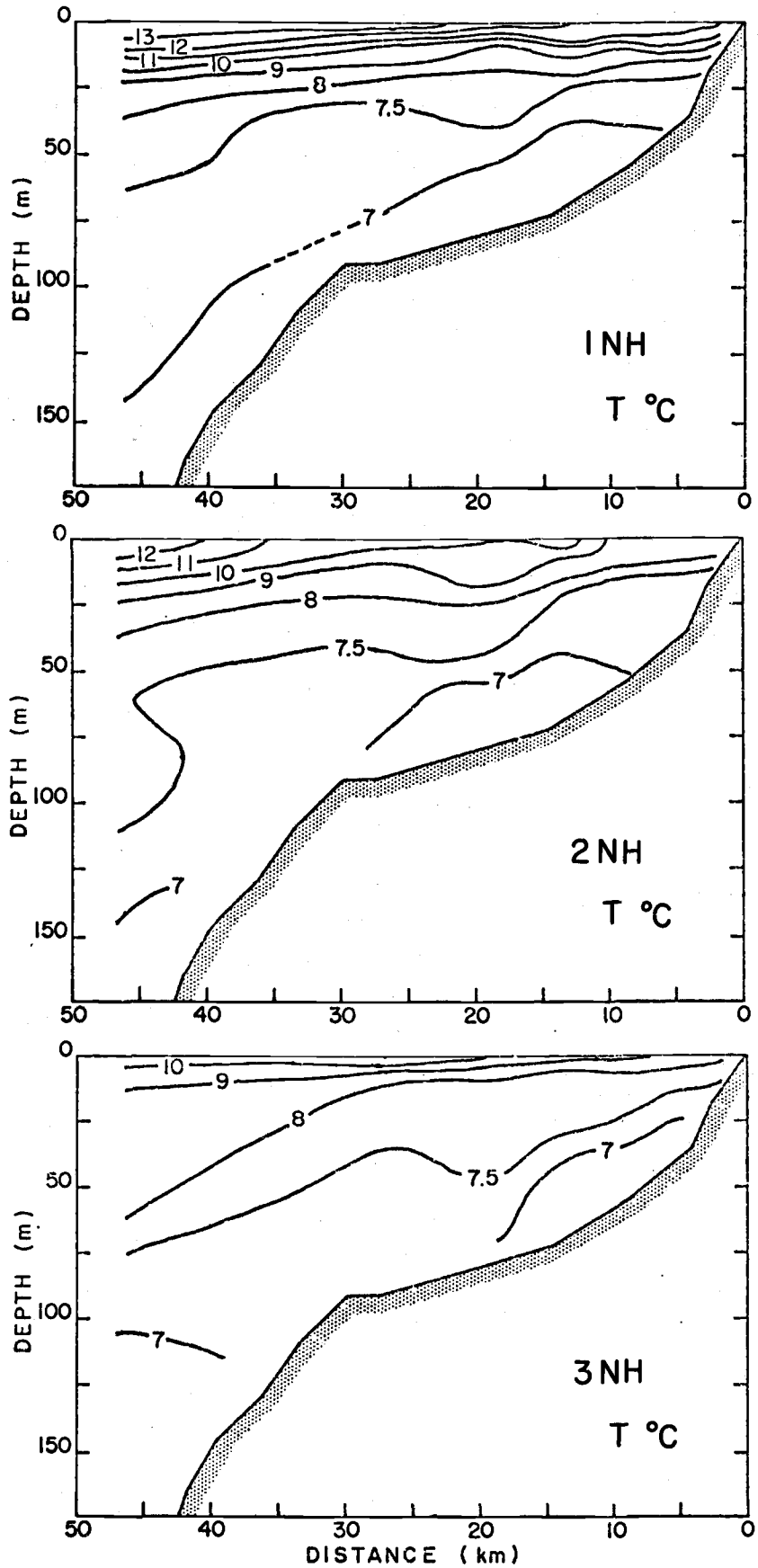

Figure 7. Vertical sections of temperature (°C) on the Newport hydrographic line.

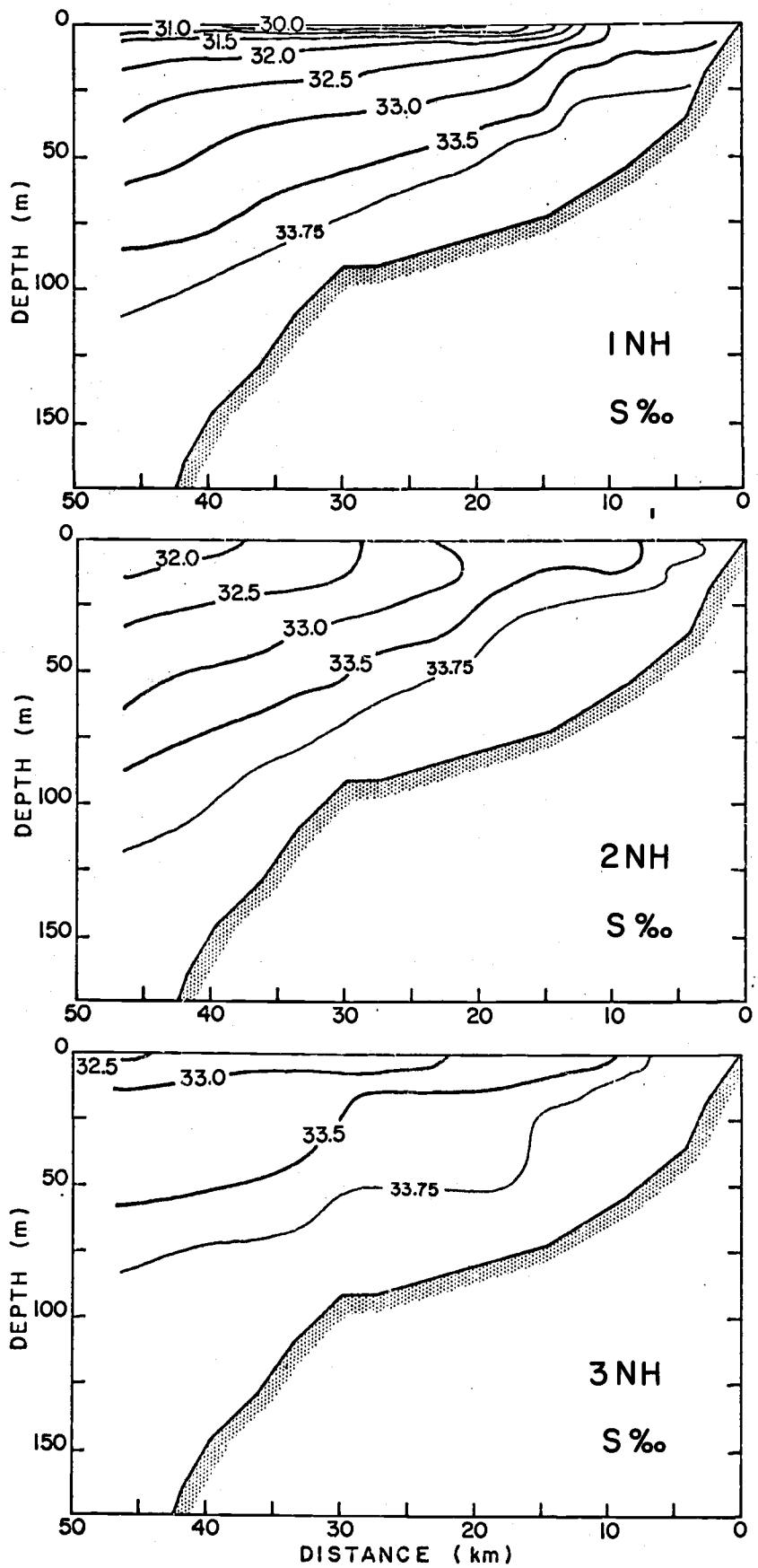

Figure 8. Vertical sections of salinity (‰) on the Newport hydrographic line.

This influence extends only to about 5-10 m depth. Minimum salinities are less than 30.5‰ at the surface. A dramatic change, similar to that seen in the temperature distribution, is observed between 1NH and 2NH. Most affected are the inshore and surface patterns. Salinities > 33.5‰ are found inshore of 2NH-5, and waters < 32‰ are limited to the surface waters past 2NH-20. The seasonal halocline seen in the 1NH section is absent along 2NH. Changes between 2NH and 3NH are not so dramatic as those between 1 and 2NH. In the region offshore of NH-15 the 33‰ isohaline has risen a maximum of ~ 40 m (at NH 25) and has assumed an attitude approximately horizontal to the sea surface. The 33.5‰ isohaline has also risen, but the gradient between 33.0 and 33.5 has lessened compared to 2NH.

Sigma-t (Figure 9). The sigma-t distributions for 1-3NH follow closely the patterns described in the salinity section. Minimum sigma-t values of <22.5 are seen during 1NH which correspond to minimum salinities and maximum temperatures. The maximum surface sigma-t (25.5) during 1NH is found at 1NH-1. By 2NH, the permanent pycnocline is found approximately 15 km offshore, although it cannot clearly be delineated due to a patch of low sigma-t water around 2NH-7. (This patch was noticed in the horizontal distribution.) The surface frontal zone has remained in approximately the same position by the time of 3NH. Relatively low gradients of sigma-t with depth are seen at about 25-50 m, one area located between 3NH-20-25

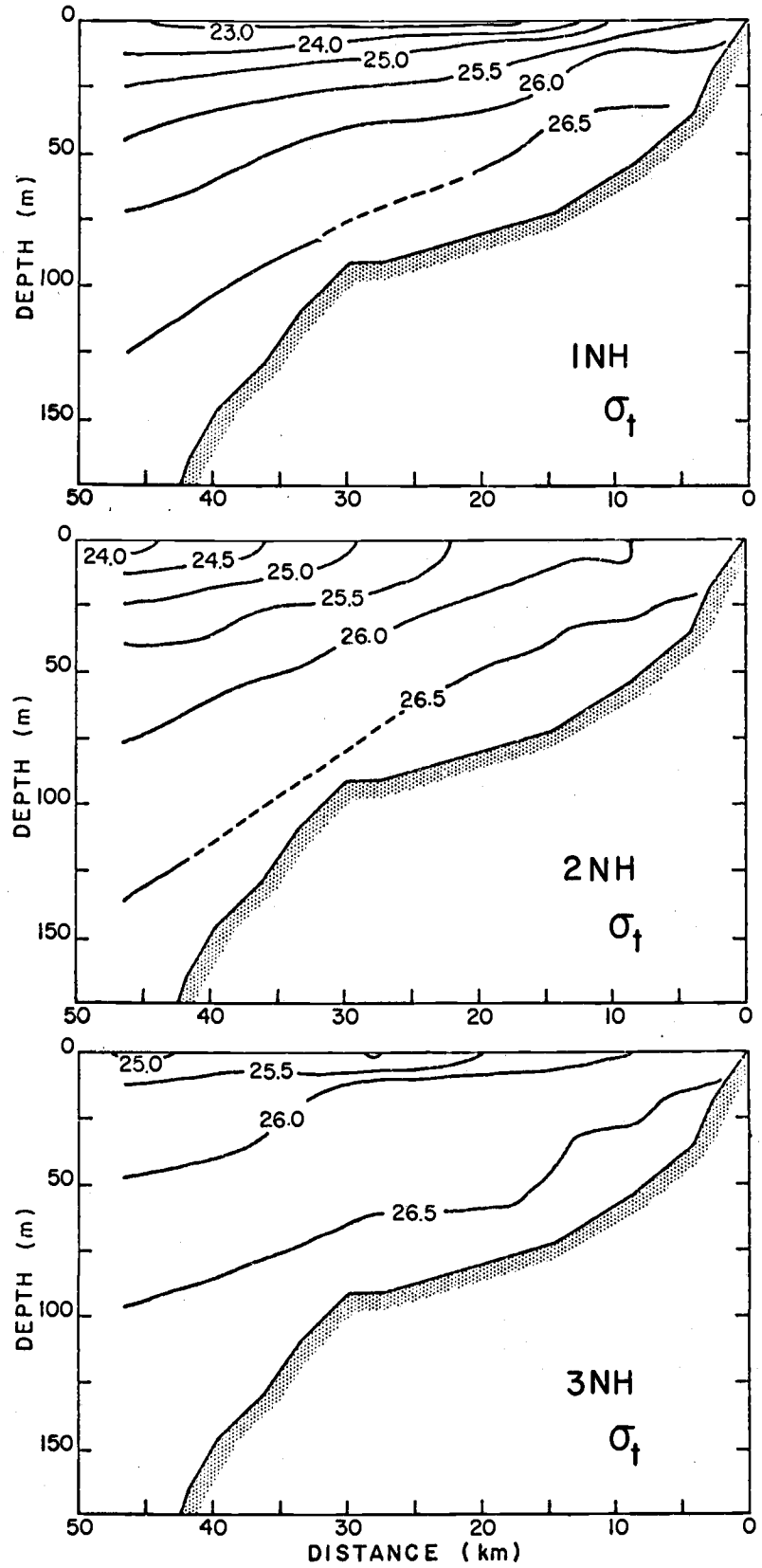

Figure 9. Vertical sections of sigma-t on the Newport hydrographic line.

and one between 3NH-10-15. These are, respectively, in the region of and below the permanent pycnocline.

Oxygen (Figure 10). The oxygen distribution differs from the distribution of temperature and salinity. A patch of water with a very high oxygen concentration (> 9 ml/l) is observed at ~10-15 km offshore during 1NH. It is in this same area that the highest gradient of oxygen with depth is recorded (~ 0.7 ml O_2/l per meter). In Figure 10, it should be noted that over most of the section there is a slight subsurface maximum at about 4 m. The difference between the surface and 4 m oxygen concentrations is on the order of 0.3 ml/l.

Again, surface and inshore changes are quite pronounced between 1NH and 2NH. Inshore surface oxygen concentrations have dropped by approximately 4 ml/l. Indeed, the entire water column at 2NH-1 and -3 shows a marked change. During 1NH the oxygen concentration ranged from ~ 7.4-3.0 ml/l, but during 2NH the range fell to ~ 3.7-2.2 ml/l. The slight subsurface maximum observed in the first section is not seen during 2NH.

A general increase in surface oxygen concentrations is observed in the 3NH section. A high gradient zone is now observed ~ 30 km offshore, and, as noted in the sections on temperature and salinity, an intrusion of deeper water is seen offshore. At 2NH-25, the 3 ml/l isogram is uplifted about 50 m. Oxygen inversions are seen at ~ 15 m at 3NH-5 and -7. These will be discussed more fully later.

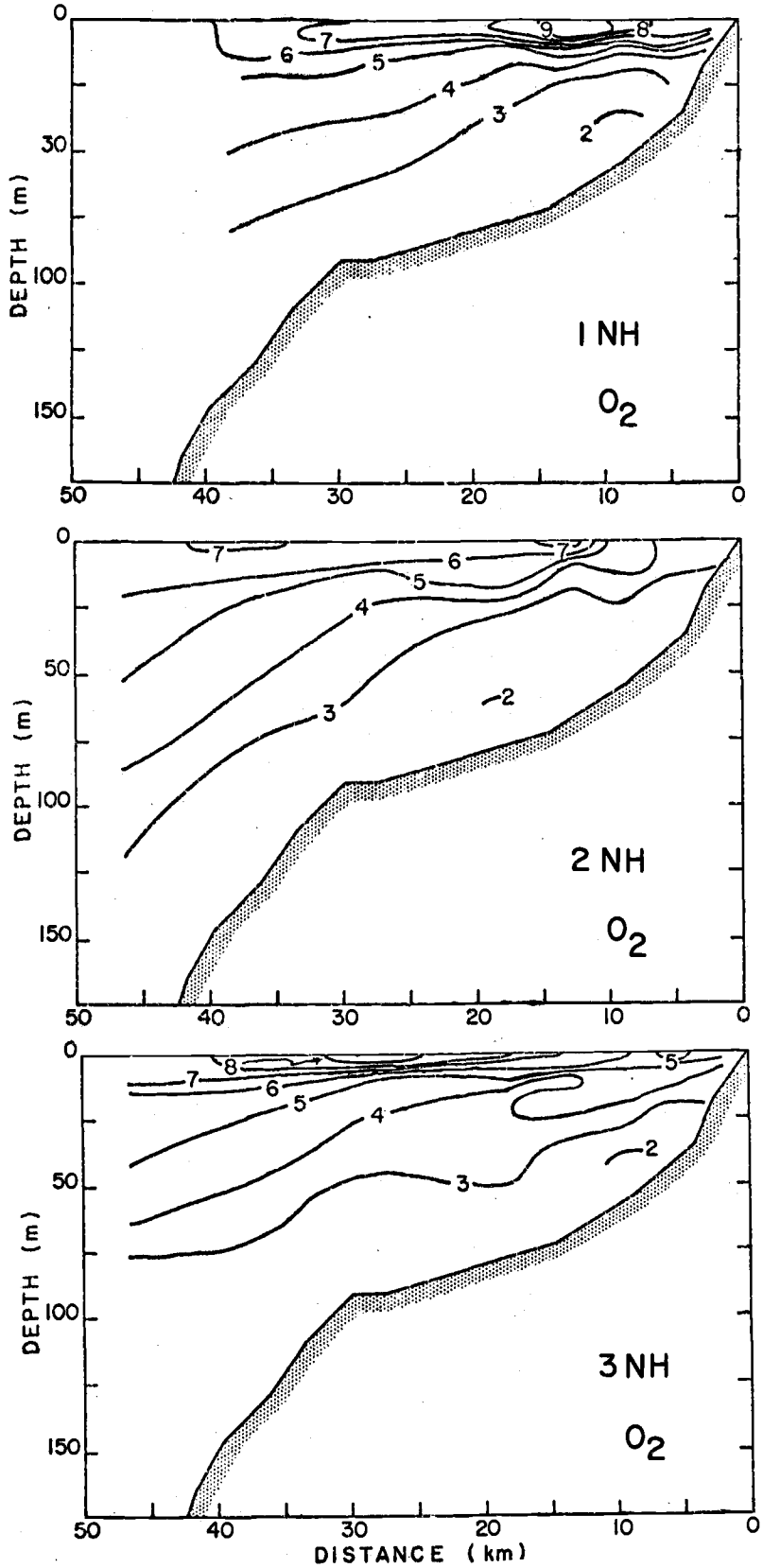

Figure 10. Vertical sections of dissolved oxygen concentrations (ml/l) on the Newport hydrographic line.

Nitrate (Figure 11). Near-zero nitrate concentrations are observed in the surface waters of the 1NH section. Maximum concentrations at the surface reach only 0.4 μM NO_3. The highest nitrate gradient with depth occurs at NH-3, about 5 km shoreward of the highest oxygen gradient. The nitrate concentration in this gradient zone changes ~ 9 μM/m. By 2NH, this high gradient zone has been uplifted and appears as a "nutrient front" 10-15 km from shore. Surface concentrations at 2NH-1 have increased by nearly 30 μM, but 2NH-7 nitrate concentrations at the surface are found to be anomalously low compared to adjacent values. While a general increase in nitrate is seen in the surface waters at 3NH-20 and -25, surface layer concentrations have decreased somewhat inshore on the 3NH section. The interior of the 3NH section shows a generally higher nitrate content compared to 2NH. For example, the 20 μM NO_3 contour has risen by ~ 10 m at 20-30 km offshore and by ~ 25 m further offshore.

Silicate (Figure 12). The silicate distribution shows much the same pattern as the nitrate distribution. However, there are some differences. The 1NH section indicates higher silicate concentrations in the offshore surface waters (compared to surface values inshore). Also a slight subsurface minimum (ΔSiO_4 ~ 5 μM) exists at ~ 4-7 m offshore of 1NH-10. This minimum is in the region of the seasonal halocline. Otherwise, the distribution of silicate generally parallels that of nitrate.

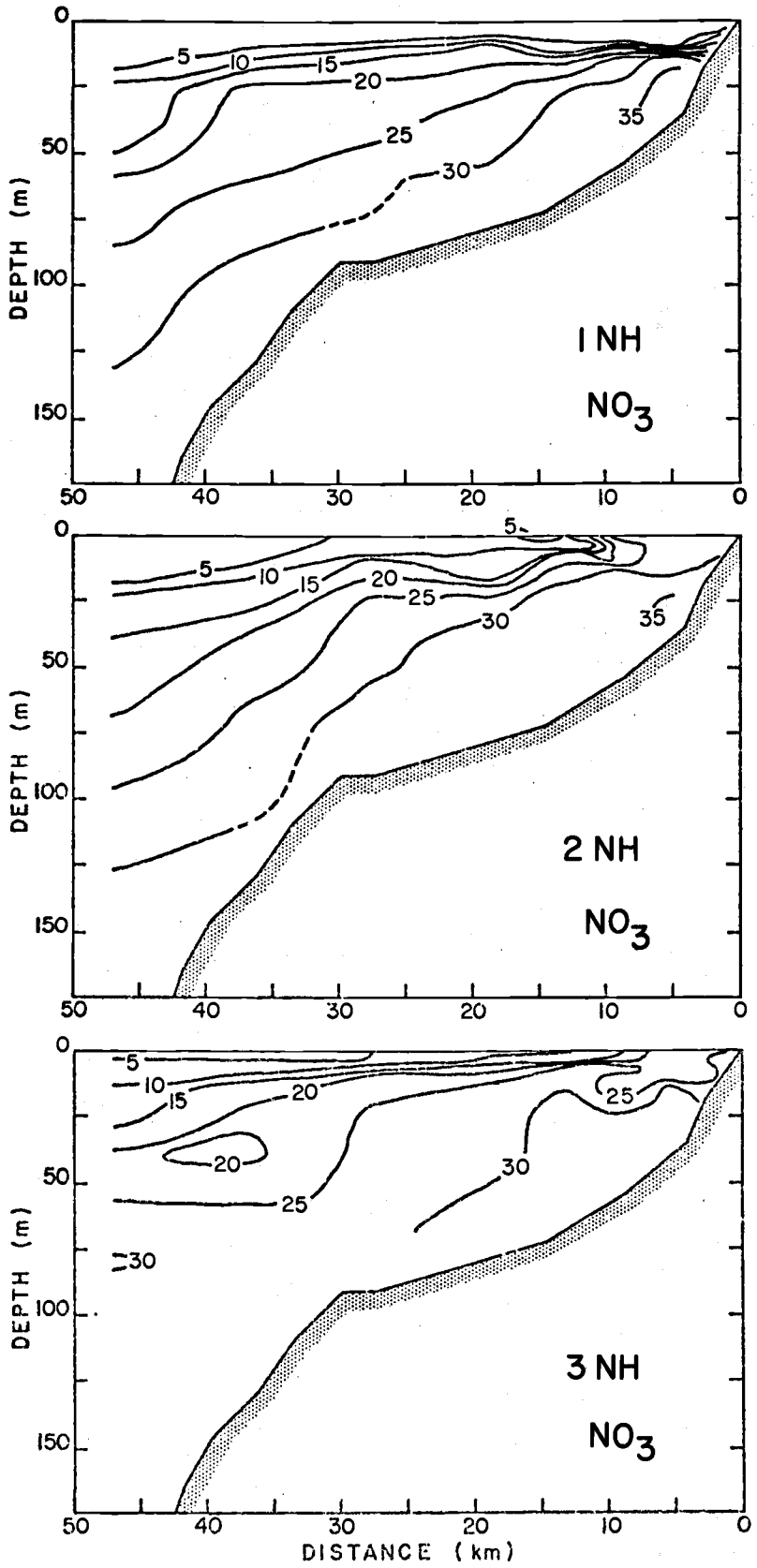

Figure 11. Vertical sections of nitrate (μM) on the Newport hydrographic line.

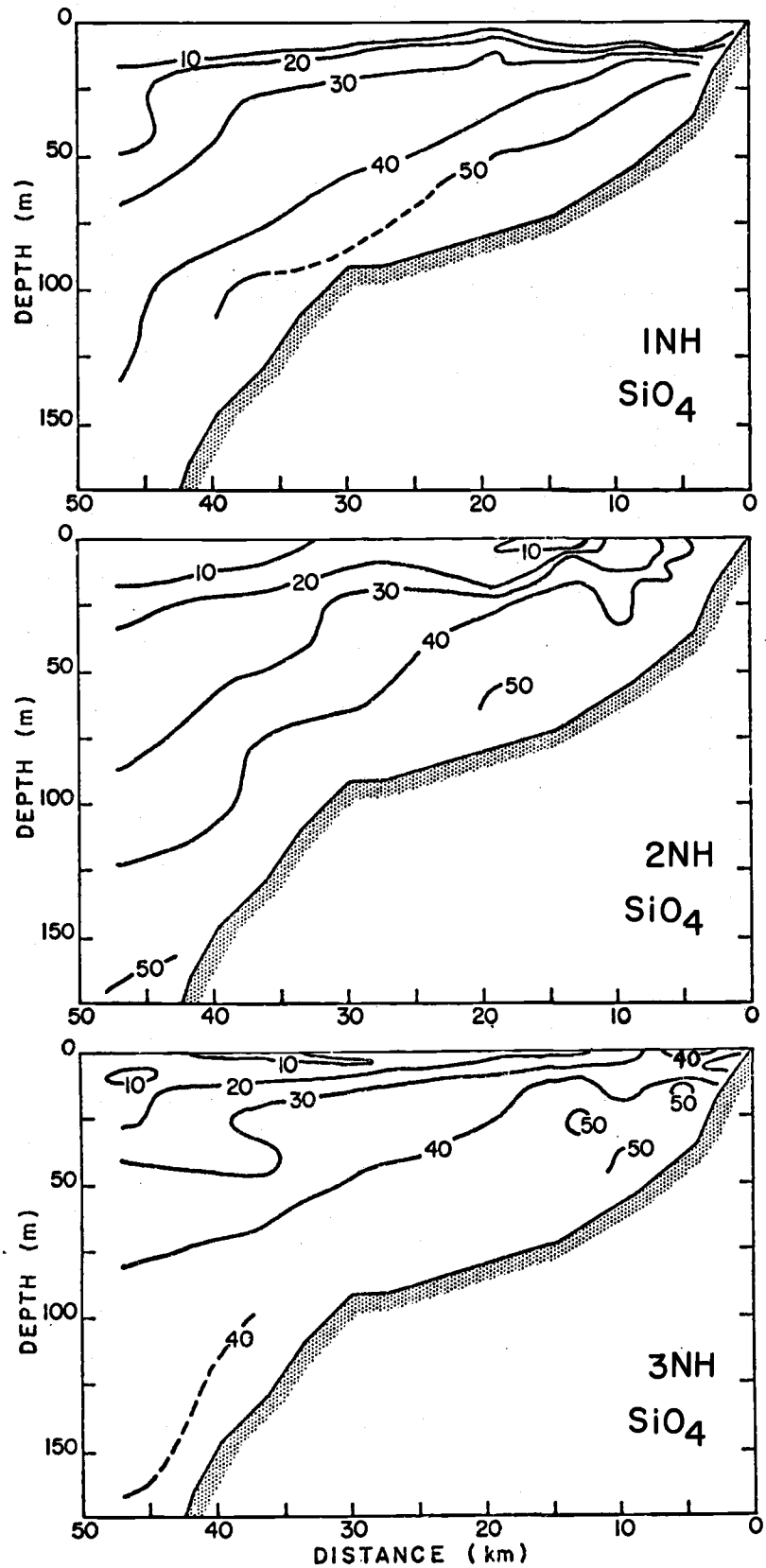

Figure 12. Vertical sections of silicate (μM) on the Newport hydrographic line.

Phosphate. Phosphate distributions are described in the section on AOU-PO_4 relationships. In general, the PO_4 distribution for 1-3NH follows the other nutrient distributions.

pH (Figure 13). (Note that no surface pH data were taken.) The pH distribution is most similar to the oxygen distribution. The very high pH (8.4) water corresponds to the maximum in oxygen seen during 1NH. The higher pH values are moved offshore in the next section, while water having a pH of about 7.8 is observed throughout the entire water column at 2NH-1. Water of this pH is typical of that found at ~ 100-150 m at NH-25. Inshore pH's remain low (< 7.9) during 3NH. Slightly higher pH values in the surface layers are found closer to shore during 3NH compared to 2NH. This follows the trend observed in the oxygen distribution.

Alkalinity and total CO_2 (not pictured). Both alkalinity and total CO_2 usually increase with depth off the Oregon coast (Park, 1968). The range for alkalinity seen on the NH line during Y7006A is 2.05-2.30 meq/l in the upper 200 m. The total CO_2 ranged from 1.83-2.28 mM. As with the other parameters described above, typical deeper water values were observed inshore on 2NH, with typical surface water values being found further offshore.

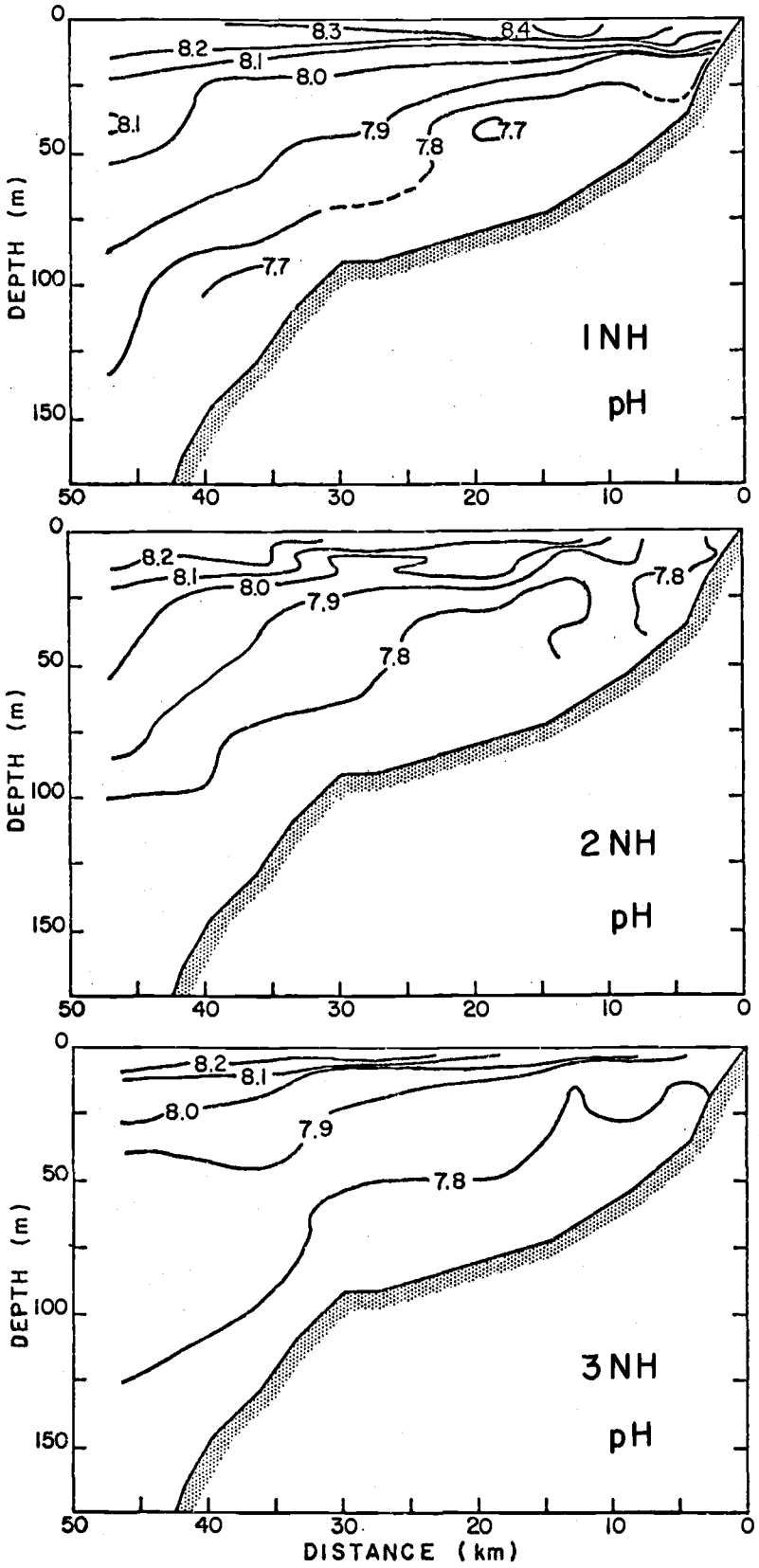

Figure 13. Vertical sections of pH on the Newport hydrographic line.

Discussion

The most outstanding feature of the sections presented above is the rapid change in the chemical and physical distributions. This change occurred more or less in two stages. The observed change between the first and second running of the Newport line was primarily evident in the surface and nearshore waters. Between the second and final occupation of the Newport line, there were noticeable alterations in the distributions away from the surface. A more graphic illustration of changes at the surface is given in Figure 14. One can see from this figure that the most pronounced changes occurred between 1NH and 2NH. For example, oxygen changed as rapidly as 1 ml O_2/l per day, and temperature changed by ~ 1° C/day. Work currently being done off the Oregon coast (CUE, 1972) indicates that the observed changes are not atypical of the upwelling regime off Oregon. One also notices that the most profound effect on the biological variables (O_2 and nutrients) occurs inshore of NH-7 (~ 13 km) while the temperature and sigma-t distributions are affected strongly over the entire distance. (Salinity, not shown, closely follows the sigma-t distribution.) This difference is the result of Columbia River water. The presence of Columbia River water offshore during 1NH is seen also in the vertical sections presented above. It is characterized by low salinity, high temperature water. A slight

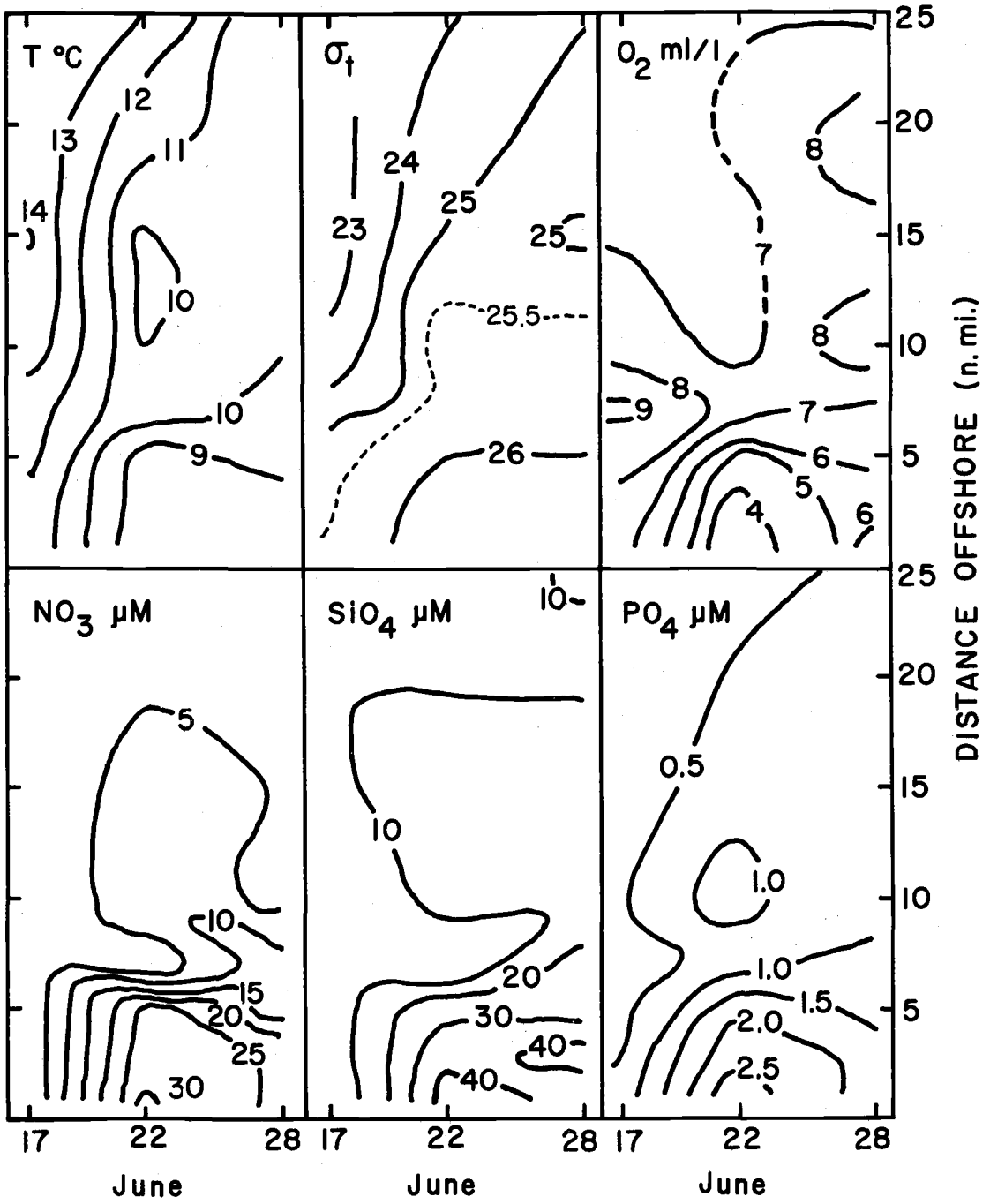

Figure 14. Temporal changes of several variables at the surface on the Newport hydrographic line.

subsurface minimum observed in the silicate distribution is another indicator of Columbia River water (Cissell, 1969).

Biological activity is quite intense during 1NH. Surface layer nutrient values are minimal ($PO_4 < 0.5$ μM, $SiO_4 < 10$ μM and $NO_3 <$ 2 μM), and oxygen concentrations of >9 ml/l are noted. Indeed, the entire region from 1NH-1 to 1NH-20 is supersaturated with respect to atmospheric oxygen. Phytoplankton activity is, then, undifferentiated between Columbia River water and coastal ocean water so that large changes in biological parameters will be noticed only in the area of freshly upwelled water. The maximum phytoplankton activity (estimated from the highest O_2 concentration), however, is located quite close to the intersection of the seasonal pycnocline with the surface. Whether this coincidence is due to chance or to nutrient enrichment of the surface waters from relatively enhanced vertical mixing is impossible to say.

Three days of moderately strong northerly winds (see Figure 5) were sufficient to significantly alter the chemical and physical distributions from those observed during 1NH. The largest changes occurred in the surface layer (~ 0-20 m) and in the region inshore of NH-7. Evidences of Columbia River plume water are practically absent from the 2NH section. This water has been transported offshore, and has been replaced by water from the inshore region, while the waters inshore have been replenished by deeper waters.

(The lack of much change away from the surface and inshore can be seen also in the T-S relationships shown later in Figure 23.)

The continuation of strong northerly winds further strengthened the upwelling between 2NH and 3NH. The bulk of water in the interior of the 3NH section became cool, high salinity water. But, while the salinity of the surface waters at the inshore stations increased some ($\sim$0.08‰) between 2NH and 3NH, the temperature increased slightly and the chemical parameters indicated renewed biological activity (oxygen increase and nutrient decrease). This can be explained with reference to the wind diagram (Figure 5). Approximately two days before 3NH, the winds shifted direction for one day, then remained as light northerlies through the period of 3NH. These last few days of "non-upwelling" winds apparently lessened the vertical mixing near the surface and allowed thermal stratification to commence. At the same time, the high nutrient input to the surface layers was used as a nutrient source for phytoplankton growth. During 1NH, the surface layers were depleted in nutrients, and phytoplankton growth was apparently nutrient-limited. The additional source of nutrients brought into the surface layers by upwelling would likely trigger phytoplankton activity. So, between 2NH and 3NH, temperature and salinity show only moderate changes. Biologically-controlled variables, on the other hand, changed considerably (especially inshore). This confirms that the biology is a quite sensitive indicator of

changes during upwelling. If upwelling occurs in a periodic succession of pulses, rather than in a steady flow, a combination of physical and biologically-controlled variables (e.g., oxygen and nutrients) might be useful in accurately pinpointing the stage of upwelling.

To use the vertical sections above as an example (see Figures 8 and 10), first consider the changes observed inshore between 2-3NH; both salinity and oxygen had increased. The salinity change alone might indicate a stronger upwelling. This may have been the case several days after the 2NH line was sampled, but, if the above interpretation is correct, upwelling had begun to lag enough so that renewed biological activity could begin inshore. So, because of the different response times between biological action and water movement, a more accurate representation of the state of upwelling is obtained. (It should be noted that this comparison could not be made if the biological response time was much greater than that of water motion.) This approach would be most useful in time scales of several days to perhaps several weeks. There may be longer (monthly, seasonal, etc.) cycles which would add confusion to comparisons over time spans greater than several weeks.

Gordon (1973) presented average source-water values for upwelling from a cruise in June, 1968. He compared his values to mean values which he extracted from the work of Pillsbury (1972) and Pattullo and Denner (1965). Approximate source-water values for this

cruise are given in Table 3 and compared with the values tabulated by Gordon (1973).

Table 3. Approximate characteristics of upwelling water.

	This work	Gordon (1973)	Pillsbury (1972)	Pattullo and Denner (1965)
Temperature	~7° C	7.8° C	8° C	8.5° C
Salinity	33.9‰	33.2‰	33.5‰	33.5‰
Sigma-t	26.5	26	26	26
Dissolved oxygen	2.5 ml/l	4 ml/l	---	---
pH	7.75	7.95	---	---
Nitrate	35 μM	---	---	---
Phosphate	2.4 μM	---	---	---
Silicate	45 μM	---	---	---

These are fairly subjective estimates. Gordon (1973) attempted to locate unmodified water near the surface inshore and follow that water approximately 100 km offshore along a constant sigma-t surface. He then read values at the appropriate depth for other variables from vertical sections.

In this work, what appeared to be unmodified water was approximated from the temperature-salinity and oxygen-salinity relationships during 2NH (Figure 23). Once these values were obtained, other variables were approximated using a calculated linear least-squares relationship between oxygen and each other variable (pH and nutrients). Phosphate was also estimated graphically from contours on a sigma-t-

horizontal distance field (see section on AOU-PO_4-preformed PO_4). This compared well with the calculated estimate.

In all cases, the estimates from this work show values more characteristic of deeper waters off the Oregon coast. This is because data obtained by Pillsbury (1972) and Pattullo and Denner (1965) did not cover the area inshore of 10 km. Thus, water they were describing had probably been altered by heating and mixing. It appears, too, that Gordon (1973) had chosen a somewhat modified upwelled water. Upwelling water comes from below the permanent pycnocline, which characteristically includes sigma-t 26.0 in its lower boundary. So, source water should be characterized by sigma-t values greater than 26.

Undoubtedly, there are year to year variations in the characteristics of upwelling water. Source water will likely reflect conditions of the previous winter and spring. Comparisons are best made against mean values. Unfortunately, data has only recently begun to be collected inshore of 10 km. As has been mentioned by others (e.g. Mooers et al., 1972; Gordon, 1973), the upwelling water usually arrives at the surface close inshore. This was also seen in the sections presented above.

Other features should be noted about the sections presented above. One is the possibility of a nutrient trap. Because of the estuarine-like circulation during upwelling (Redfield et al., 1963,

p. 66), nutrients may accumulate in high velocity shear zone between the onshore and offshore moving waters. Turbulent mixing in this zone, however, might destroy such a trap. Alternately, in shallow areas organic detritus might sink to the shelf bottom and be remineralized by bacteria in the sediments. This would be another form of nutrient trap and would enhance the nutrient supply to the surface layers. Such a nutrient trap off the Oregon coast was suggested by Gordon (1973) in his analysis of the carbon dioxide system during upwelling. He noted that the isograms of P_{CO_2} were more steeply inclined than the isopycnals. This indicated a carbon supply on the shelf bottom. Calvert and Price (1971) compared nutrient-salinity relationships in the upwelling region off the southwest coast of Africa. They found that nutrient concentrations at a given salinity were higher on the shelf area than further offshore. For Y7006A, a similar comparison was made (see later section on AOU, PO_4, and preformed PO_4). To summarize conclusions from that comparison, indications are present of nutrient regeneration on the shelf.

Another important feature of the above vertical sections is the appearance of temperature inversions, both inshore and offshore. Discussion of this feature is given in the section on oxygen, temperature and salinity.

Velocity Distribution on the Newport Hydrographic Line

Results

Following the procedure outlined by Smith et al. (1966) onshore transports and velocities were computed from the salinity distribution during three occupations of the Newport hydrographic line during Y7006A (Figure 8). Assumptions for the purposes of calculation were that no heat, salt, or water was transported across any isogram. Longshore gradients were assumed to be negligible. Given these assumptions, a decrease in the area between two isograms can be interpreted as a net offshore transport per unit meridional length. Smith et al. (1966) present a velocity section based on the mean of the velocities calculated independently for both temperature and salinity. Examination of the present data, and consideration of the time interval between occupations of the hydrographic line (approximately 86 hours and 176 hours, respectively), showed that the assumption of no heat transport across isograms was clearly being violated. Thus, what is presented here is the result of calculations based on the salinity distribution alone.

The velocity distribution presented in Figure 15a is calculated from the salinity distributions found on the Newport line on the 17th and 21st of June. The level of no zonal motion corresponds closely to a sigma-t value of 26.0. Collins (1964) found that

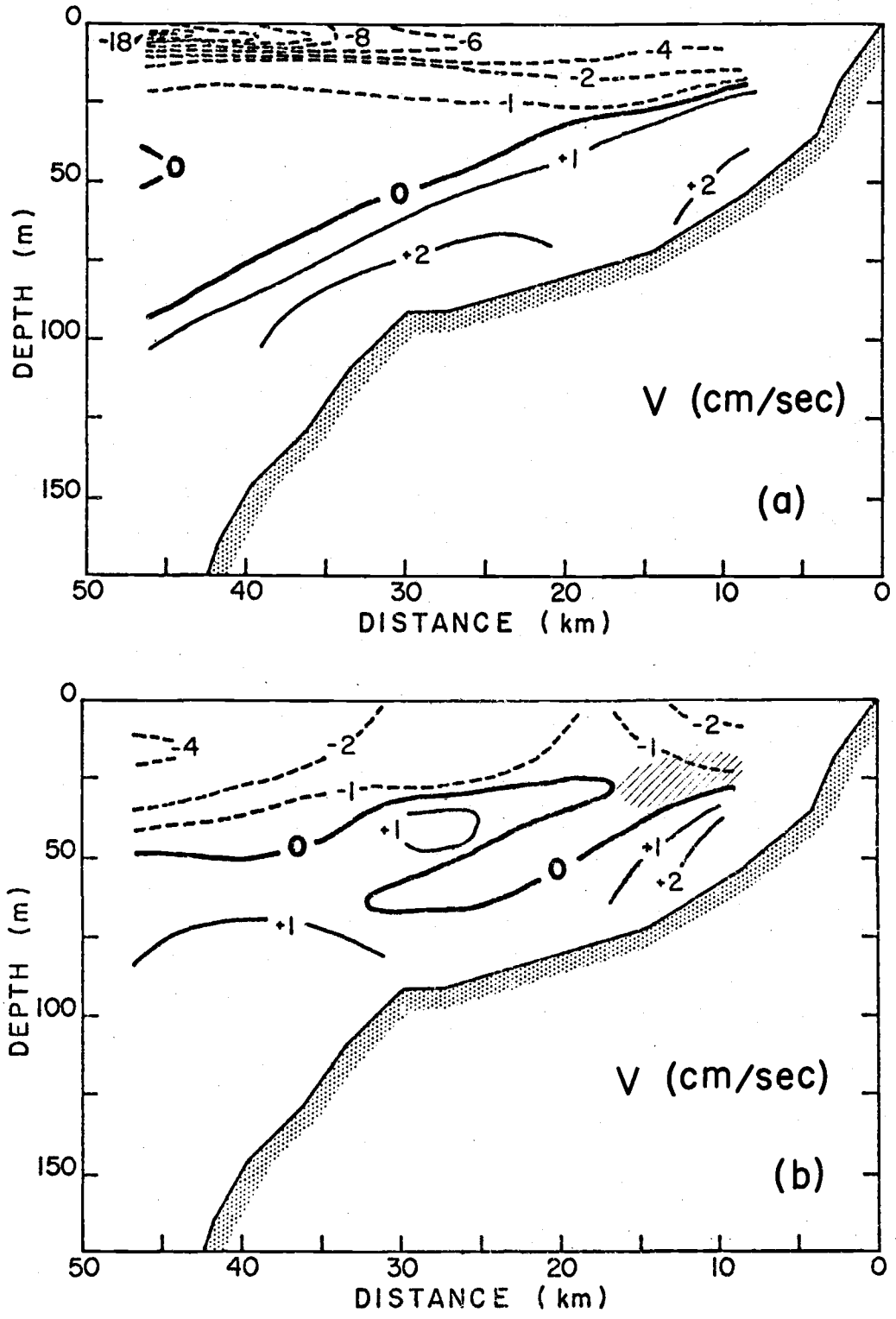

Figure 15. Onshore velocity (cm/sec) computed from the salinity distribution for: a) 1-2NH and b) 2-3NH. Dotted lines indicate offshore flow; solid lines indicate onshore flow.

water with a sigma-t of 26.0 is always in the lower part of the permanent pycnocline. Seaward of 30 km, there is a slight minimum in offshore velocity in the upper part of the permanent pycnocline (~ sigma-t 25.5). Maximum onshore velocities were slightly less than 2 cm/sec, averaging about 1 cm/sec. Maximum offshore velocities exceeded 18 cm/sec, and the average offshore velocity was computed to be about 6 cm/sec.

This picture differs in some respects from that presented by Smith et al. (1966). They found the level of no zonal motion to coincide with the upper layer of the permanent pycnocline, and they observed a minimum offshore velocity at about 25 m. While the maximum offshore velocity they computed is approximately one-third that calculated for this case, the maximum onshore velocity they computed is nearly twice that found here. The general features, however, are comparable.

A slightly different velocity structure is calculated from the salinity distributions on the 21st and 28th of June (Figure 15b). Noticeably different is a parcel of water moving offshore into a region of predominantly onshore flow. Offshore velocities have diminished compared to the first section, while onshore velocities have remained nearly the same.

The tongue of water moving offshore corresponds approximately to water with a sigma-t of 26.3. This is somewhat below the perma-

nent pycnocline. The shaded area in Figure 15b represents a local temperature inversion. (See section on O_2-T-S and Figure 16.) This inversion is likely generated by insolation of salty upwelled water and subsequent sinking of this water below the permanent pycnocline (Mooers et al., 1972). The inversion in this case occurs at a sigma-t coinciding with that of the offshore-moving tongue of water. The velocity structure presented here, constructed independently of the temperature distribution, supports the hypothesis presented by Mooers et al. (1972).

Mass Transport

The mass transport per unit longshore width was also computed from the salinity sections. For the 86- and 176-hour period the mass transport was 3.1 and 4.7 x 10^9 gm/cm, respectively. This is the onshore transport across a 1-cm plane at NH 20 (37 km offshore). Because of the nature of the computation, total onshore transport equals total offshore transport.

These results are compared to the theoretical Ekman transport, using average daily wind data measured at South Jetty, Newport, Oregon. The daily averages were computed from hand-calculated hourly averages of the wind record (Gilbert, 1972). The north-south wind stress was computed using the formula

$$\tau_y = \rho_a C_D \left| \sqrt{u^2 + v^2} \right| v \qquad (2)$$

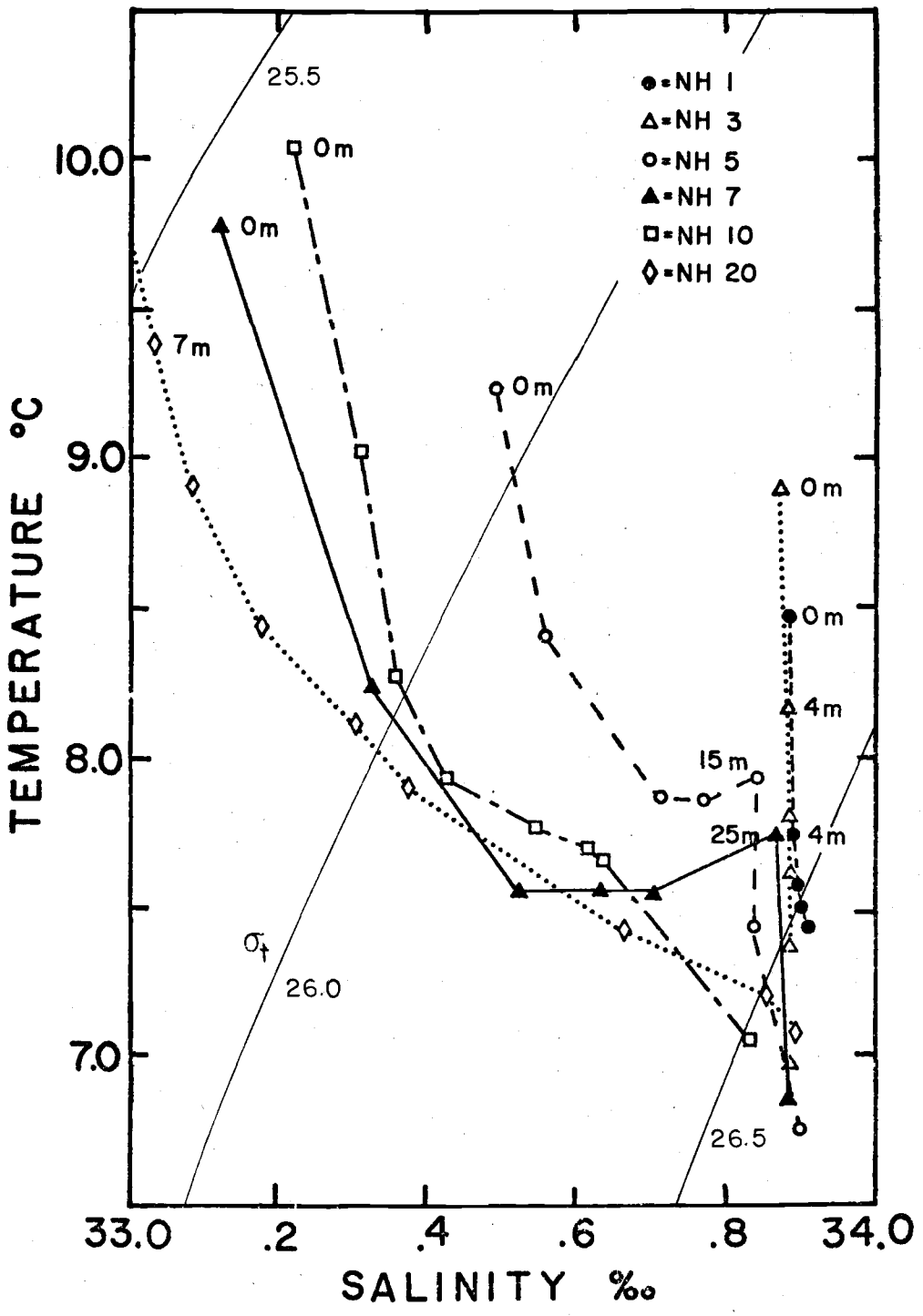

Figure 16. Temperature-salinity relationship for several stations on the 3NH line. (Note the expanded temperature scale.)

where:

ρ_a = density of air, 1.2×10^{-3} g/cm^3

C_D = drag coefficient, 2.6×10^{-3}, dimensionless

u = east-west component of wind velocity, cm/sec

v = north-south component of wind velocity, cm/sec, positive when wind is blowing from the north.

Results of this calculation show the average wind stress for the two time periods to be 0.38 and 0.29 dynes/cm^2, respectively. The offshore mass transport was then computed by

$$M_x = \overline{\tau}_y / f \qquad (3)$$

where $\overline{\tau}_y$ = the average north-south wind stress and f = the Coriolis parameter. The density of water was taken as 1.0 gm/cm^3. Results of these computations compare well with the mass transport estimated from the salinity distribution. (See Table 4.)

Table 4. Comparison of mass transport computed from salinity distribution to theoretical transport.

	from S‰ distn*	from wind stress data*
June 17-21	3.0	3.1
June 21-28	4.9	4.7

* units are X 10^9 gm/cm

These results suggest that, when averaged over several days,

the wind stress calculated from mean daily winds might be useful as a semi-quantitative indicator of mass transport during upwelling.

On the other hand, it may have just been fortuitous that the estimates of mass transport compare so well, and that it was the special conditions occurring during these times which allowed the good comparison. (Also, the drag coefficient, C_D, used in the calculation is highly uncertain.)

As can be seen from the wind data (Figure 5), the winds were northerly during the cruise, with the exception of the last few days. It has been suggested in numerical models of coastal upwelling (e.g. Hurlburt and Thompson, 1972) and by others (Mooers et al., 1972) that the decay of upwelling takes longer than the onset of upwelling. Hurlburt and Thompson indicate a continued, but reduced, upwelling even 35 days after the wind stress in their model was set equal to zero. Thus, if the wind is highly variable, estimates obtained from wind stress data may show a considerable error, because of the response time of the ocean to the effects of the winds. More comparisons, at different stages of upwelling, are necessary for stronger conclusions to be reached.

Nutrient Flow

A rough approximation of the nutrient flow can be made from the calculations derived from the salinity distribution. First it is

necessary to estimate the transport of that water which returns offshore by subsurface flow. (This is the water characterized by the temperature inversion.) Calculations show this volume to be approximately 10-25% of the total offshore transport. This value, coupled with average concentrations of nutrients in upwelling waters, can give an estimate of the nutrient flow. Averaged over the entire period covered by the three occupations of the Newport line, the following results are obtained (calling average source water 2.4 μM PO_4, 34 μM NO_3, 44 μM SiO_4, and using $\rho_{sea} = 1.0$):

	Onshore Transport (moles/day/cm)	Returned via Sinking (moles/day/cm)
Phosphate	1.7	0.2-0.4
Nitrate	22	2-5
Silicate	38	4-10

It should be noted that these are very crude estimates, maybe within a factor of 3-5. For this reason estimates of utilization based on average concentrations in the total offshore flow are not made.

CHAPTER FOUR

CHEMICAL RELATIONSHIPS ON THE NEWPORT HYDROGRAPHIC LINE

AOU, PO_4, and Preformed PO_4

During the seasonal upwelling off the Oregon coast it is thought that a new water mass if formed by cold, saline water coming to the surface, moving offshore, and then sinking along or near the base of the permanent pycnocline (Mooers et al., 1972). (The permanent pycnocline is defined as water in the sigma-t range, 25.5 to 26.0 (Collins, 1964).) As the upwelled water moves along the surface it is warmed and slightly freshened by mixing with surface waters, and it is also warmed by solar radiation. This water is still more dense than the surface waters offshore. The sinking water is characterized by a temperature inversion (Mooers et al., 1972, and others), and has also been observed to have a turbidity maximum, arising from biological activity when it was at the surface (Pak et al., 1970).

Upwelled water is characterized by the following chemical parameters: low oxygen, high nutrients, high alkalinity, low pH (Park et al., 1962), and high P_{CO_2} (Gordon, 1973). Only changes in oxygen and nutrients, specifically phosphate, in the upwelled water

will be considered here. For deep and intermediate waters, apparent oxygen utilization and preformed phosphate have been used in conjunction with temperature and salinity to trace water masses (Pytkowicz and Kester, 1966; Pytkowicz, 1968). The use of these latter two parameters in an upwelling regime will be evaluated here.

Apparent oxygen utilization (AOU) has been defined (Redfield, 1942) as $O_2' - O_2$, where O_2' is the saturation value of oxygen at the in situ temperature and salinity; and O_2 is the measured dissolved oxygen concentration. In a parcel of deep water AOU changes only as a result of mixing and biological activity. If one wishes to closely examine and compare AOU distributions in surface waters the following factors must also be taken into account: in situ temperature changes, oxygen exchange with the atmosphere, and, to a lesser extent, barometric pressure and relative humidity changes. Relative magnitudes of the major effects will be reviewed later.

Preformed phosphate is calculated from the measured phosphate concentration and the AOU (Redfield, 1942) according to:

$$P.PO_4 = PO_4 - a(AOU) \qquad (4)$$

where: $P.PO_4$ = calculated preformed phosphate

PO_4 = measured dissolved inorganic phosphate

a = "Redfield's ratio" (= 1/138 when AOU and PO_4 are expressed in molar units)

AOU = apparent oxygen utilization

Classically, preformed phosphate approximates the phosphate concentration present in a parcel of water at the time it sank from the surface, assuming its dissolved oxygen had equilibrated with the atmosphere. Preformed phosphate is a conservative property of seawater, ignoring changes due to dissolution or precipitation of phosphatic minerals.

To be able to extend this concept to the evaluation of $P.PO_4$ distributions in surface and near surface waters, the mathematical formulation of $P.PO_4$ (Equation 4) should be employed. That is, preformed phosphate is defined as that phosphate present in the water at zero AOU. The classical conceptualization of $P.PO_4$ is adequate and has been shown to be valid (Pytkowicz, 1971) when dealing with deep and intermediate waters, considering the situation at the point of origin of the deep and intermediate water masses. In surface waters off Oregon during the upwelling season the assumption of air-sea equilibrium is hardly ever met, and the question remains of defining the "surface." Is this the sea surface, or is it the bottom of the euphotic zone? A parcel of water may rise to the surface, change its measured phosphate concentration, and sink, now with a different phosphate concentration. It may, though, still have the same value of preformed phosphate. It should be made clear that the only mechanisms for changing preformed phosphate, aside from mixing, are exchange of heat and/or oxygen with the atmosphere. This

assumes that "Redfield's ratio" remains constant. (Evaporation and precipitation will also alter preformed phosphate. This effect however, can be ignored over short time periods.) Said another way, changes in preformed phosphate values at the surface arise only from achievement of oxygen equilibrium through exchange processes across the air-sea interface. As such, preformed phosphate can serve as an indicator of exchange processes, in a limited geographical area, rather than its more classical use in conjunction with water mass characterization. This use is similar to the integration technique used by Pytkowicz (1964) and Redfield (1948) in their determination of oxygen exchange rates.

The latter way of looking at preformed phosphate distributions also relieves the apparently paradoxical situation arising in waters supersaturated with oxygen. In this case the AOU takes a negative value, yielding a value of preformed phosphate greater than the measured value of phosphate (see Equation 4). The difference between measured and preformed phosphate under this condition has been called apparent phosphate utilization (APU) by others (Stefansson and Richards, 1963).

For a water mass, resulting only from the mixing of two water types of different salinities, the preformed phosphate value will be constant, when normalized to constant salinity (Alvarez-Borrego, 1973). A plot of $P.PO_4$ versus salinity will yield a straight line

relationship. The change in the normalized phosphate concentration from the preformed value indicates changes due to biological activity. Near-surface changes in the normalized preformed phosphate concentration are indicative of exchange of oxygen and/or heat across the sea surface.

We will now consider the effect of various processes on a parcel of water which upwells and subsequently sinks.

Heating and photosynthesis only. As this water is rising to the surface, it is being warmed. This decreases the solubility of oxygen, and consequently AOU will decrease. Calculated values of preformed phosphate will thus show an increase (Equation 4). A change in temperature of 2.8°C (7°-9.8°C, at S = 33.5‰) will change the AOU by 20 μM. This is equivalent to a 0.15 μM change in the preformed phosphate value. As the water enters the euphotic zone, photosynthesis begins, causing a reduction in nutrient concentrations and a corresponding increase in oxygen. (The order in which this sequence occurs can be reversed with no effect on the argument.) The change due to photosynthesis can be expressed as $\Delta PO_4/\Delta O_2$ = constant = (1/138). The preformed phosphate value does not change if this ratio remains constant.

Exchange included. In the case where undersaturated water rises to the surface and undergoes oxygen exchange with the atmosphere, the direction of this exchange is expected to be from the atmosphere to the

water. AOU in this case will decrease, but there will be no corresponding decrease in nutrient concentrations. A calculation of preformed phosphate will show an increase (= a(ΔAOU), see Equation 4). Assuming that the rate of exchange of oxygen is proportional to the difference between actual and equilibrium concentrations of oxygen, exchange will be decreased as the water is being heated.

Mixing included. Care must be taken when applying AOU to mixtures of waters (Pytkowicz and Kester, 1966; Pytkowicz, 1971). The oxygen concentration of the mixture will be $\Sigma f_i O_{2_i}$, where f_i is the fraction of the ith water type in the mixture, and O_{2_i} is the oxygen concentration of the ith water type. But as oxygen saturation is not a linear function of temperature and salinity the AOU of mixture will not necessarily be $\Sigma f_i AOU_i$. A case typical off the Oregon coast might be that a water (W_1) of T = 7.0°C, S = 33.5‰, O_2 = 2.5 ml/l mixes with water (W_2) of T = 10°C, S = 29.0‰, O_2 = 7.55 ml/l in a ratio of 2/3 W_1 to 1/3 W_2. (These values and ratios are close to those suggested by Mooers et al. (1972) as a possible mixture forming the temperature inversion layer seen during upwelling.) The individual AOU's are 4.32 and -0.99 ml/l, respectively. For this case the AOU calculated for the mixture from the separate AOU's is within 0.01 ml/l of the AOU computed from the resultant temperature, salinity, and oxygen values of the mixture of the two waters. This is within the precision of O_2 measurements and thus negligible. This shows that a more extreme

difference in temperatures and salinities than found in this upwelling regime is necessary to yield any significant difference in AOU's of mixtures resulting from the nonlinearity of oxygen solubility.

Results

Vertical sections of AOU, PO_4, and preformed PO_4 on the Newport line are presented in Figures 17-19. Isopleths are presented on a depth versus horizontal distance field as well as on a sigma-t versus horizontal distance field. This latter method of presentation is given to offer some idea of how a variable relates to the trajectory of a water parcel (Redfield et al., 1963). In general water will flow along an isentropic surface. This type of surface is closely approximated by a surface of constant sigma-t. This means that a horizontal vector on a sigma-t distance field will indicate the trajectory of a parcel of water. However there are some drawbacks. Near the surface the effect of winds, insolation, and evaporation or precipitation will predominate. The original interpretation is, in this case, not generally useful. For the most part diverging, converging, or non-horizontal isograms on a sigma-t distance field will indicate the effect of in-situ processes on a chemical distribution. Conservative parameters will be indicated by parallel, horizontal isograms.

Newport line. 17-18 June. The upper 10 m from NH-1

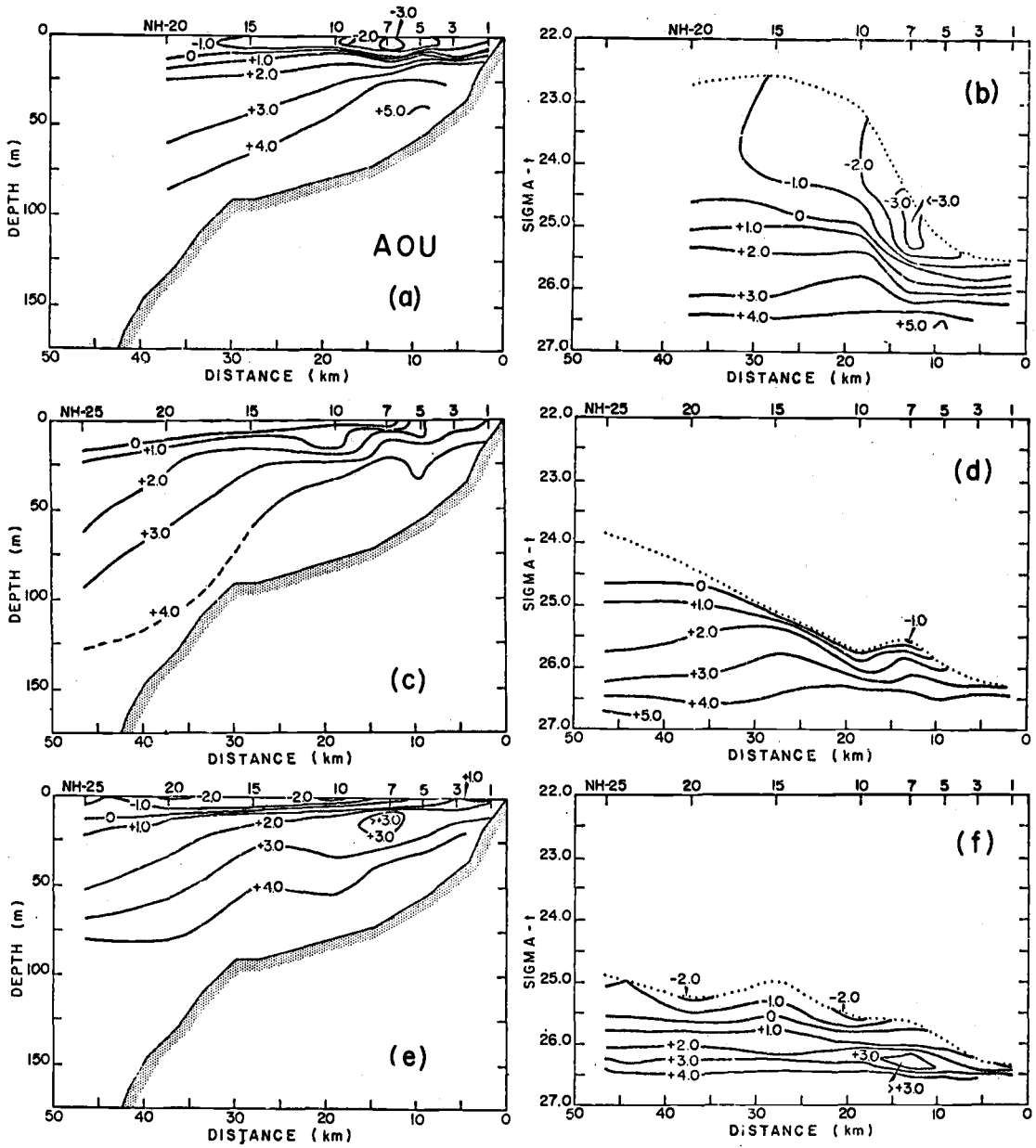

Figure 17. Vertical sections of apparent oxygen utilization (ml/l) for 1NH (a), 2NH (c), and 3NH (e), and plots of AOU for the same lines on a horizontal distance-sigma-t field for 1NH (b), 2NH (d), and 3NH (f). The dotted line indicates the sea surface.

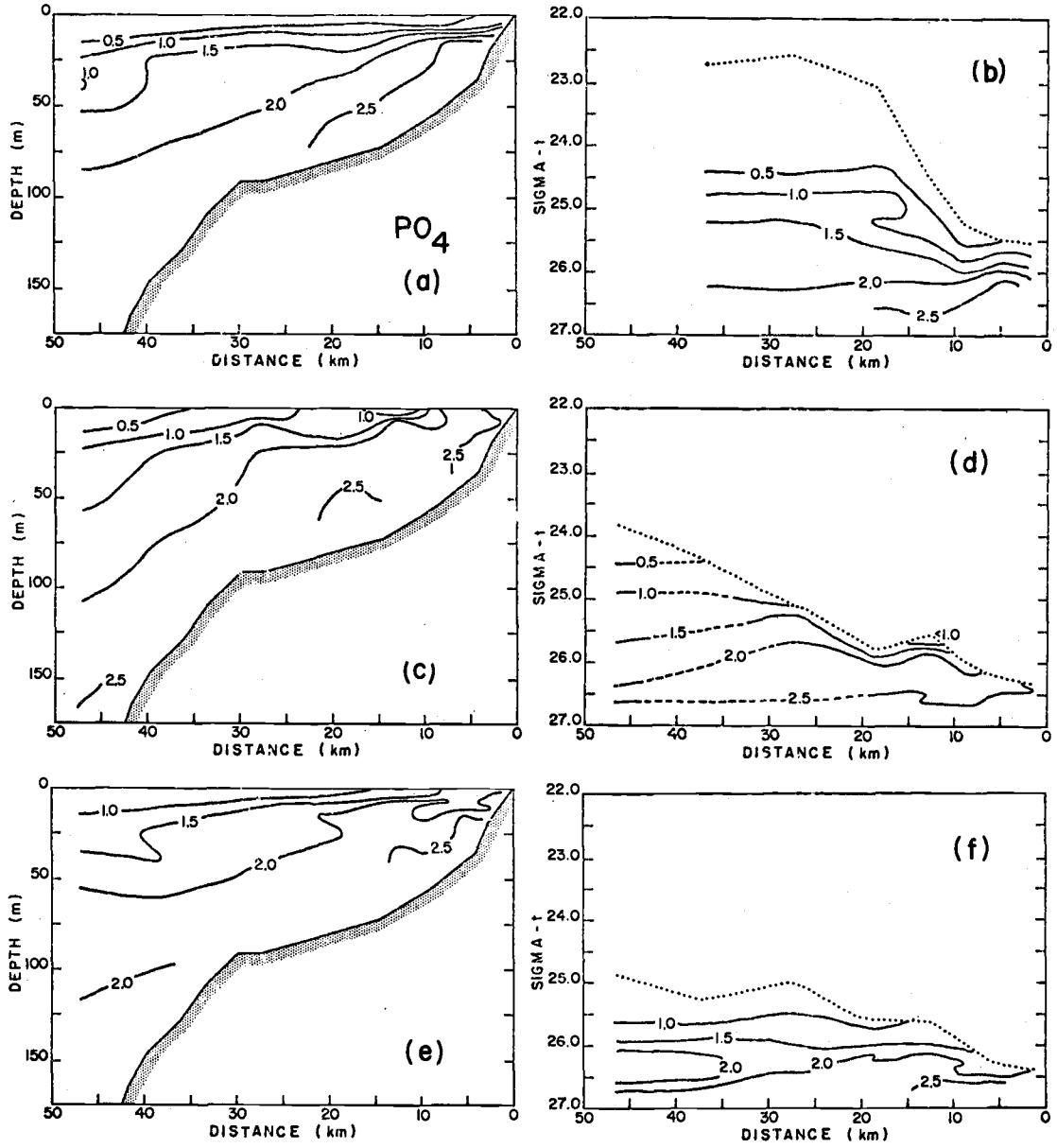

Figure 18. Vertical sections of phosphate (μM) for 1NH (a), 2NH (c), and 3NH (e), and plots of PO_4 for the same lines on a horizontal distance-sigma-t field for 1NH (b), 2NH (d), and 3NH (f). The dotted line indicates the sea surface.

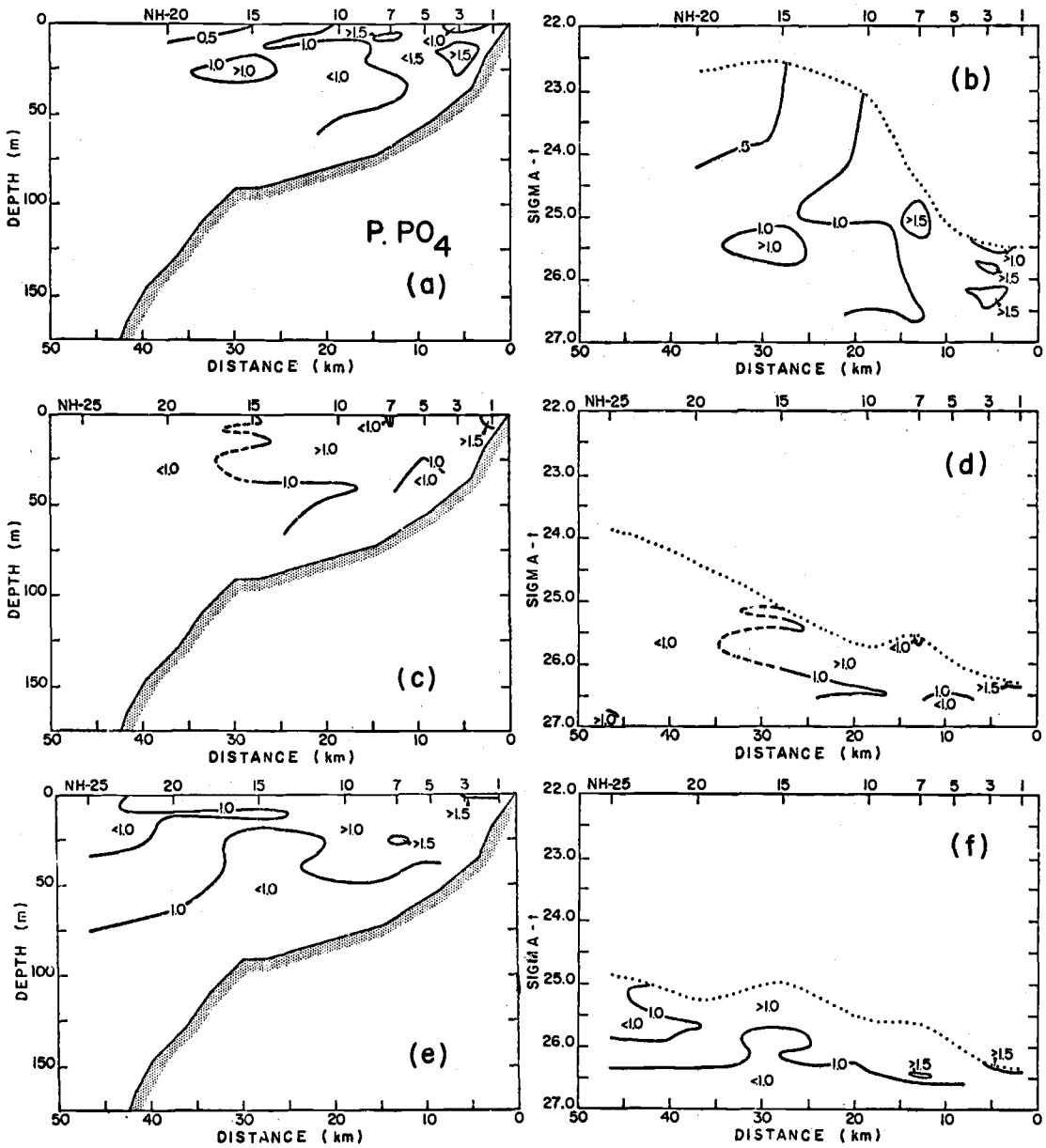

Figure 19. Vertical sections of preformed phosphate (μM) for 1NH (a), 2NH (c) and 3NH (e), and plots of $P.PO_4$ for the same lines on a horizontal distance-sigma-t field for 1NH (b), 2NH (d), and 3NH (f). The dotted line indicates the sea surface.

to NH-20 are supersaturated with oxygen, having a minimum AOU of less than -3 ml/l around NH-7 (Figure 17a, b). This is the result of strong photosynthetic activity. The phosphate concentration is less than 0.5 μM in the surface layer, although the minimum values occur in the region offshore of NH-15 (Figure 18a, b). This area is most strongly affected by Columbia River water. The highest value of AOU, 5 ml/l, is found near the bottom (~ 40 m) at NH-5. High phosphate concentrations, around 2.8 μM. are located in this same area. It appears that phosphate concentrations for a given value of AOU are higher at NH-1, and below 15 m at NH-3, than elsewhere along the line.

The strong density gradient at the surface between NH-10 and NH-3 (see Figure 9) is the result of a high salinity gradient, and relatively uniform warming of the surface layers. At NH-10, the 11° C isotherm is approximately associated with the 32‰ isohaline, while further inshore this isotherm is associated with a salinity of 34.4‰. The AOU and PO_4 isopleths correspond closely to the shape of the isotherms (not shown). Values of AOU, PO_4, T, and S are nearly constant along the 26.5 isopycnal, although the PO_4 isograms slope upward inshore. The values are close to 4.1 ml/l, 2.3 μM, 7° C, and 33.8‰, respectively.

Preformed phosphate varies considerably (Figure 19a, b). Variations do not, however, correlate well with sigma-t. Maximum

values of 1.5 μM are found in the region of NH-3 (below 10 m). A minimum of 0.3 μM preformed PO_4 is found at the surface at NH-20. There appears to be a general trend toward decreasing values of preformed PO_4 with distance from shore.

Newport line. 22 June. The surface layers have become undersaturated with respect to oxygen from the coast to 15 km from shore (Figure 17c, d). A maximum value of 3.0 ml/l AOU is found at NH-1, decreasing to a minimum of -1.0 ml/l at NH-7. The highest surface gradient (~ 3 ml/l) occurs between NH-5 and NH-7 and it corresponds closely to the surface density front (where the sigma-t's 25.5 and 26.0 are found at the surface). At NH-20, the AOU-sigma-t (compare Figure 17b and 17d) correspondence is approximately the same as that found during the first run of the Newport line. Also, values in the front and closer to shore are roughly the same for a given sigma-t as those found six days previously. This time, however, they are at, or closer to, the surface than they were previously. A high AOU gradient with depth (2 ml/l per 3 m) is seen at NH-7 and corresponds to a high temperature gradient.

A high phosphate gradient (1.3 μM per 3 m) is noticed in the same place (Figure 18c, d). Similar to AOU the highest surface gradient in PO_4 is found in the surface density front. The maximum value of PO_4 of 2.67 μM occurs at NH-1 with a minimum of 0.27 μM at NH-25. A relative minimum (0.65 μM) is located in the region of

the AOU minimum.

The surface preformed phosphate values maintain the same general trend of decreasing concentration with distance from shore (Figure 19c, d). A maximum surface value of 1.7 μM is located at NH-1 and a minimum of 0.5 μM occurs at the surface at NH-25. There still seems to be no correlation of preformed phosphate concentration with isopycnal surfaces.

Newport line. 28 June. The zero AOU isopleth is found at the surface at about 12 km from shore, and the waters have remained undersaturated shoreward (Figure 17e, f). The surface waters, however, are found to have decreased in AOU, having a minimum of -2.3 ml/l at NH-10. The maximum surface value of 1.2 ml/l is located at NH-3. An interesting feature is an apparent patch of high AOU (~ 3 ml/l) water located between about 5 and 20 m at NH-7. This will be discussed more fully later (see p. 68-70).

Surface phosphate values shoreward of NH-7 remain high, although they are lower than those observed on the 22nd of June (compare Figures 18c and 18e). Surface maxima of 1.9 μM are located at NH-1 and NH-3. The highest surface gradient is 0.7 μM/4 km located between NH-3 and NH-5, and it is associated with a density change of approximately 0.4 sigma-t units (26.3-25.9).

Preformed phosphate maintains the trend of decreasing values with distance from shore (Figure 19e, f). A surface maximum of

1.7 μM is still found at NH-1, and the minimum value of 0.8 μM is at NH-25. There appears to be a section of water with relatively high values of preformed PO_4 (~ 1.2 μM) at about 15-25 m depth (sigma-t ~ 26.4) from NH-1 through NH-10.

Discussion

Interpretation of the observed conditions is difficult owing to the extraordinarily dynamic nature of the events associated with the commencement of upwelling over this 12-day period. The great deal of advective motion of the water adds to the difficulty of interpretation. While it is the offshore transport of water which causes the most dramatic changes in the hydrographic regime, the bulk of the transport is associated with meridional flow (Collins et al., 1968). Comparison of the three sets of data for this line can be made only if there is the assumption of horizontal homogeneity over a rather broad geographical band parallelling the coast. Even during the time it takes to sample the Newport line, events may be occurring which can change the regime. Thus, an explanation based on the assumption of a synoptic picture may not be adequate. It should be realized, too, that many processes are happening simultaneously, and that the data shown will represent the balance between, or the sum of, their effects. For the purposes of this discussion, it will be assumed that, except where noted, upwelling occurred in a continuous band along the

coast, and processes acting to alter the water composition were longitudinally uniform in this band.

The change in the AOU distribution between the 17th and 22nd of June was due primarily to the advective transport of surface layer water away from the coast, and replacement of deeper water near the shore. The lighter water (< 25 sigma-t) has been moved offshore, and the permanent pycnocline has appeared as a surface front. There was little motion of the permanent pycnocline at depth in the region of NH-20 and NH-25 (compare in Figure 9). This picture is consistent with observations by others (Mooers et al., 1972) that the newly upwelled water is confined to a narrow band (~ 10 km) near the coast.

The apparent patch of high AOU water seen in Figure 17e, f is interpreted as a section of deeper water broken off from water of similar AOU by a tongue of water of relatively low AOU. This tongue of water is further characterized by a temperature inversion, and appears to be the beginnings of the new water mass formed during upwelling. Temperature-salinity characteristics suggest that the origin of this water is the near surface layer at NH-1 and NH-3 (Figure 16). It seems clear from the T-S diagram that the low AOU water is formed not by mixing but rather by a combination of warming, photosynthesis, and aeration of the undersaturated water. (If anything, the AOU minimum layer will be lessened as it mixes with

the higher AOU water beneath the surface.) The change in temperature at the inversion is small ($\sim 0.25°C$), so that there will be little effect on the O_2 solubility; thus warming effects on AOU can be ignored.

A plot of AOU (or O_2) versus PO_4 will indicate to what extent the minimum in AOU is due to photosynthetic activity, and to what extent it is due to air-sea exchange. This is shown in Figure 20. It appears that at NH-7 the minimum AOU is almost exclusively the result of aeration of the water, while at NH-3 and NH-5 it is due primarily to photosynthetic activity. This can be seen from the process vectors indicated on the figure. It should be noted that there is no temperature inversion observed at NH-3. A possible explanation of the observed data is that the first water reaching the surface had sunk before any photosynthesis could commence, and that equilibrium was being obtained by air-sea exchange. As photosynthesis started and as the water was further warmed, the tendency for air-sea exchange lessened. The water closer to the shore would have a relative AOU minimum more characteristic of photosynthesis.

The preformed phosphate shows a subsurface maximum in the temperature inversion at NH-7 which is comparable in magnitude to surface values at NH-1. This is further evidence for the hypothesis of water mass formation in the near coastal region. Alternatively, the preformed PO_4 maximum could be the result of advection of high

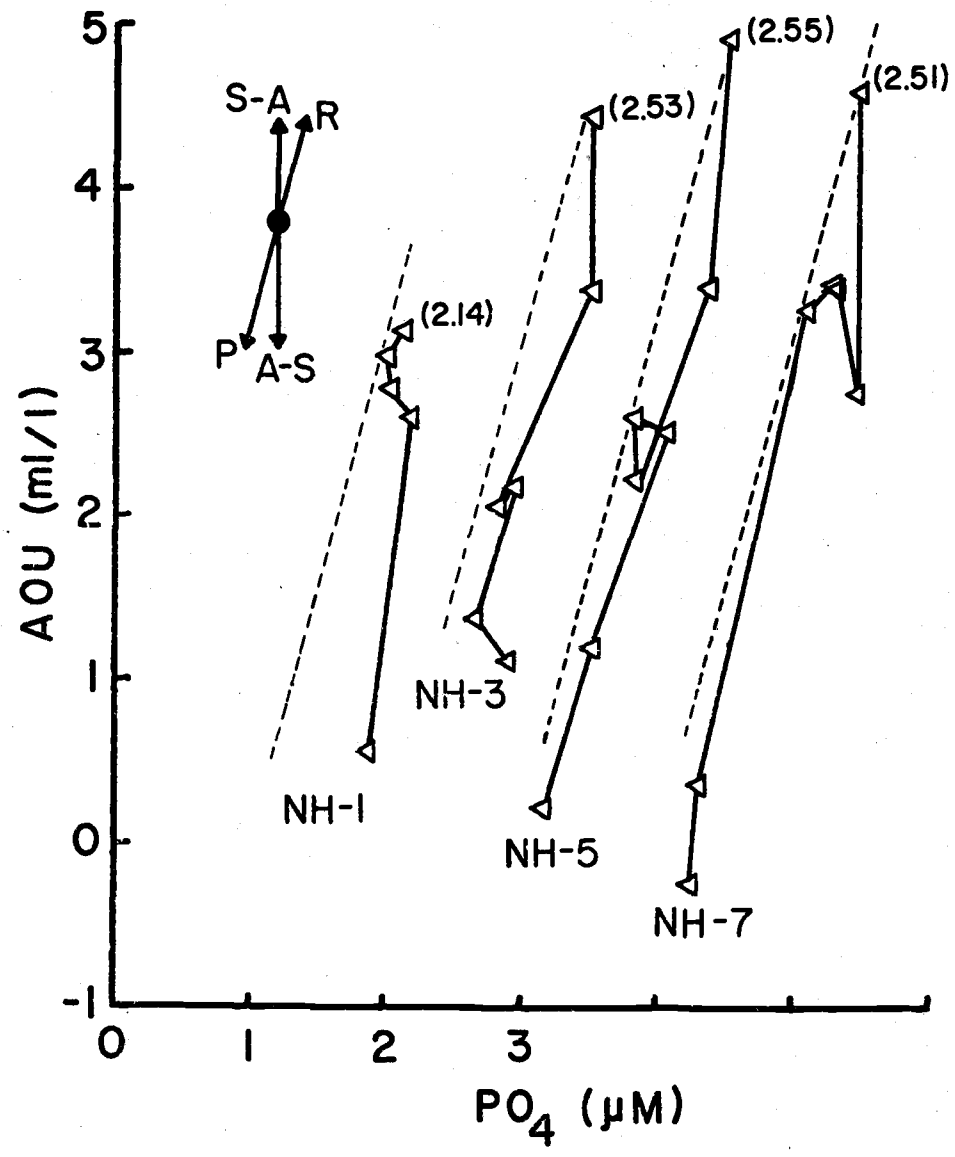

Figure 20. Apparent oxygen utilization versus phosphate for several inshore stations on 3NH. (Note that each successive station is offset by 1μM PO_4. The PO_4 concentration of the deepest point is given in parentheses.) Process vectors are P = photosynthesis, R = respiration, S-A = oxygen transfer from sea to air, A-S = oxygen transfer from air to sea. The theoretical slope (= 3.09, see text) is shown by a dashed line for respiration/decay and photosynthesis and is referenced to AOU = 0, PO_4 = 1 μM.

$P.PO_4$ water to the surface, and subsequent sinking. If so, this water must have been previously subjected to aeration (or heating). There is evidence of an upwelling event prior to this cruise which could account for the high preformed phosphate by the mechanisms described above (see p. 19).

Surface preformed phosphate follows the same trend as seen for the surface sigma-t's. This is the expected result of offshore movement of surface water. It should be noted, though, that for a given sigma-t the preformed phosphate value inshore is higher than that offshore. Temperature effects are not great enough to account for the entire difference. This would indicate that the inshore regime is affected by oxygen transfer from the atmosphere to the water. A plot of preformed phosphate versus salinity for different stations is shown in Figure 21. This figure gives an indication of the relative effects of warming and air-sea exchange on the changes in the preformed phosphate concentration.

The lack of correlation between preformed phosphate and sigma-t seen in Figure 19 is also noteworthy. This lack of correlation indicates primarily the effect of air-sea exchange of oxygen in altering the preformed phosphate concentrations.

The diagrams of PO_4 and AOU on the sigma-t-distance field, as mentioned earlier, will indicate <u>in situ</u> chemical processes. Specifically, these isograms should bend upward in the case of

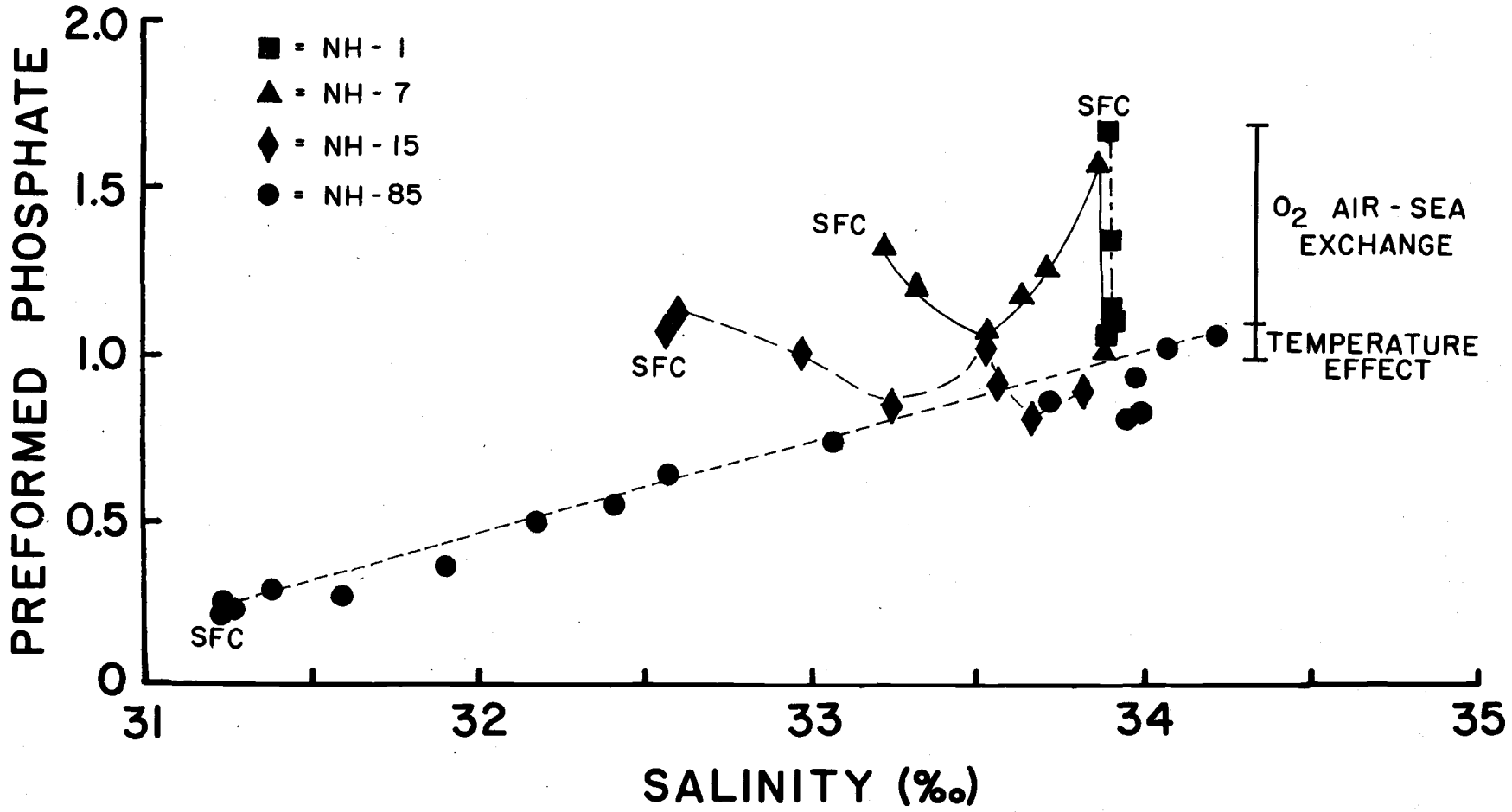

Figure 21. Preformed phosphate (μM) versus salinity (‰) for several stations on 3NH. Note the effect of air-sea exchange on the inshore distributions.

nutrient regeneration in the sediments. Isograms of AOU are more difficult to interpret because AOU is affected by gas exchange and temperature and salinity affect both AOU and sigma-t. For this reason, only isograms of PO_4 will be considered. As can be seen in Figure 18b, the inshore stations have a higher PO_4 concentration at a given sigma-t than further offshore. (A comparison of PO_4-salinity relationships shows the same feature.) This is to be expected if there is a nutrient source low in the water column. This trend continues during 2NH (Figure 18d), although it is not so pronounced near the bottom. The 2.0 μM isogram, however, does show an upward trend between 40 km offshore and the coast. This possibly indicates diffusion of high nutrient bottom waters into the water column. By 3NH, an apparent maximum has developed offshore and relatively higher phosphate concentrations are still found inshore. This maximum, however, is due to several low PO_4 values which are probably in error. This maximum occurs deep enough in the water column (~ 100 m) so that a comparison of PO_4 to AOU can be made. If the maximum is due to nutrient regeneration, AOU should show a similar maximum (relative to adjacent values). This is not the case. So, there does seem to be evidence for nutrient regeneration on the shelf area. From the distributions seen above, it seems likely that most of this regeneration occurs in or near the sediments rather than in the water column, as in the classical estuarine-type nutrient

trap.

Difficulties with the use of preformed PO_4 and AOU as indicators of water mass formation in an upwelling region are seen in several areas. A few of these have been mentioned above. Analytical and sampling procedures for O_2 and PO_4 must be extremely good. Both values are used in the calculation of $P.PO_4$, so that errors are magnified and resolution is hampered. The possibility of patchiness and local changes in $\Delta O_2/\Delta PO_4$ add to the confusion in interpretation. These parameters, however, can be extremely valuable when used in conjunction with other hydrographic variables, e.g. sigma-t, T, and S.

Nutrient Ratios

Park (1967) suggested the use of the ratio of preformed nitrate to preformed phosphate in water mass characterization. This method would find its best use in intermediate and deep waters. At the sea surface heating and gas exchange with the atmosphere alter the calculated preformed nutrient values (see section on AOU and $P.PO_4$). This section will describe the use of measured inorganic $(NO_3 + NO_2)$: PO_4 (hereafter denoted N:P) and SiO_4:PO_4 (Si:P) ratios in the upwelling regime off Oregon. Stefansson and Richards (1963) have also mentioned these ratios in their description of waters off the Columbia River and Strait of Juan de Fuca.

According to the model of Redfield et al. (1963), when an "average oceanic organic molecule" is oxidized it will yield changes in NO_3 and PO_4 in the ratio of 16:1 (by atoms), assuming complete oxidation of ammonia. From the work of Grill and Richards (1964) and the observations of Park (1967) for the upper 200 m off Oregon, the ratio of $\Delta Si:\Delta P$ should be 23:1. These ratios do not necessarily imply, however, that the measured nutrient values will follow these ratios. Though this can be shown to be the case for "average" ocean water (Redfield et al., 1963), nutrient limitation and the effects of the Columbia River will alter the ratios in the surface coastal waters off Oregon. This has been mentioned by Hager (1969).

A linear regression of PO_4 on NO_3 and on SiO_4 was done for each time the Newport line was run. Results of the regressions are:

Regression Lines	Theoretical Slopes
1NH	
$PO_4 = 0.46(\pm.12) + .0628(\pm.006)NO_3$	$\Delta PO_4/\Delta NO_3 = .0625$
$PO_4 = 0.31(\pm.16) + .0448(\pm.006)SiO_4$	$\Delta PO_4/\Delta SiO_4 = .0435$
2NH	
$PO_4 = 0.45(\pm.10) + .0628(\pm.004)NO_3$	
$PO_4 = 0.37(\pm.10) + .0484(\pm.003)SiO_4$	
3NH	
$PO_4 = 0.32(\pm.05) + .0660(\pm.002)NO_3$	
$PO_4 = 0.10(\pm.07) + .0496(\pm.002)SiO_4$	

(Numbers in parentheses are ±2 standard errors.) The slopes of these regression lines are in close agreement with those predicted from the model. The lack of a (0, 0) intercept, however, will force the X:Y ratio to be different from $\Delta X:\Delta Y$, the slope of the line. Writing the equation in the general form $Y = mX + b$, it can be seen that as X increases $(Y/X - b/X)$ approaches $Y/X = m(=\Delta Y/\Delta X)$. This means that as nitrate, for instance, increases, N:P will approach $\Delta NO_3:\Delta PO_4$. A non-zero intercept can be interpreted in several ways. In general, it might mean that the source waters were relatively depleted in one nutrient compared to the normal assimilation ratio (N:P::16:1). Alternately, in the case of NO_3 versus PO_4, we are not measuring all the available nitrogen sources in the water column, so that a non-zero intercept (in this case indicating nitrogen depletion) would be expected.

Off the Oregon coast, nutrient concentrations generally increase with depth. There may, however, be small relative minima in the near surface waters due to photosynthesis. These will not affect the general trend of slightly increasing ratios with increasing depth if there is a non-zero intercept. Surface water, especially water in the euphotic zone, will have its nutrient ratios changed most drastically. These changes can be attributed to two main causes, the effect of the Columbia River water and NO_3 (and possibly SiO_4) depletion. Columbia River water will contribute greater proportions of silicate

relative to phosphate (Hager, 1969). In a photosynthetically active area, NO_3 may become depleted before PO_4, though the PO_4 may continue to decrease after all NO_3 is used up. Continued PO_4 depletion most possibly indicates the presence of alternate nitrogen sources, such as ammonia, urea and other excretion products, and dissolved amino acids. Nutrient ratios, then, would be expected to be useful in distinguishing older surface waters (in terms of photosynthetic activity)(low N:P). Further, Si:P ratios in the surface waters will indicate the presence of Columbia River plume waters. Columbia River influence will be characterized by a high Si:P at the surface.

Figure 22 shows N:P, Si:P, and PO_4 versus depth for all stations run during the three successive samplings of the NH-line. Notice that although the PO_4 versus depth plots indicate similar type trends as those indicated in the nutrient-ratio diagrams, the latter distinguish more clearly the difference, or similarity, between the surface and deeper waters. (Note that the depth scale in the figures extends to only 100 m.) The comparisons of the 1NH section are especially striking. The PO_4 versus depth diagram shows more or less of a scatter diagram of values above a diagonal connecting (0, 0) and approximately (100 m, 2.5 μM). Generally, the PO_4 concentration increases with depth. The N:P ratio shows the sharpest gradient between 10 and 25 m, clearly separating surface waters having an N:P ratio of 1 or less and deeper waters showing an average N:P of $\sim$ 13.

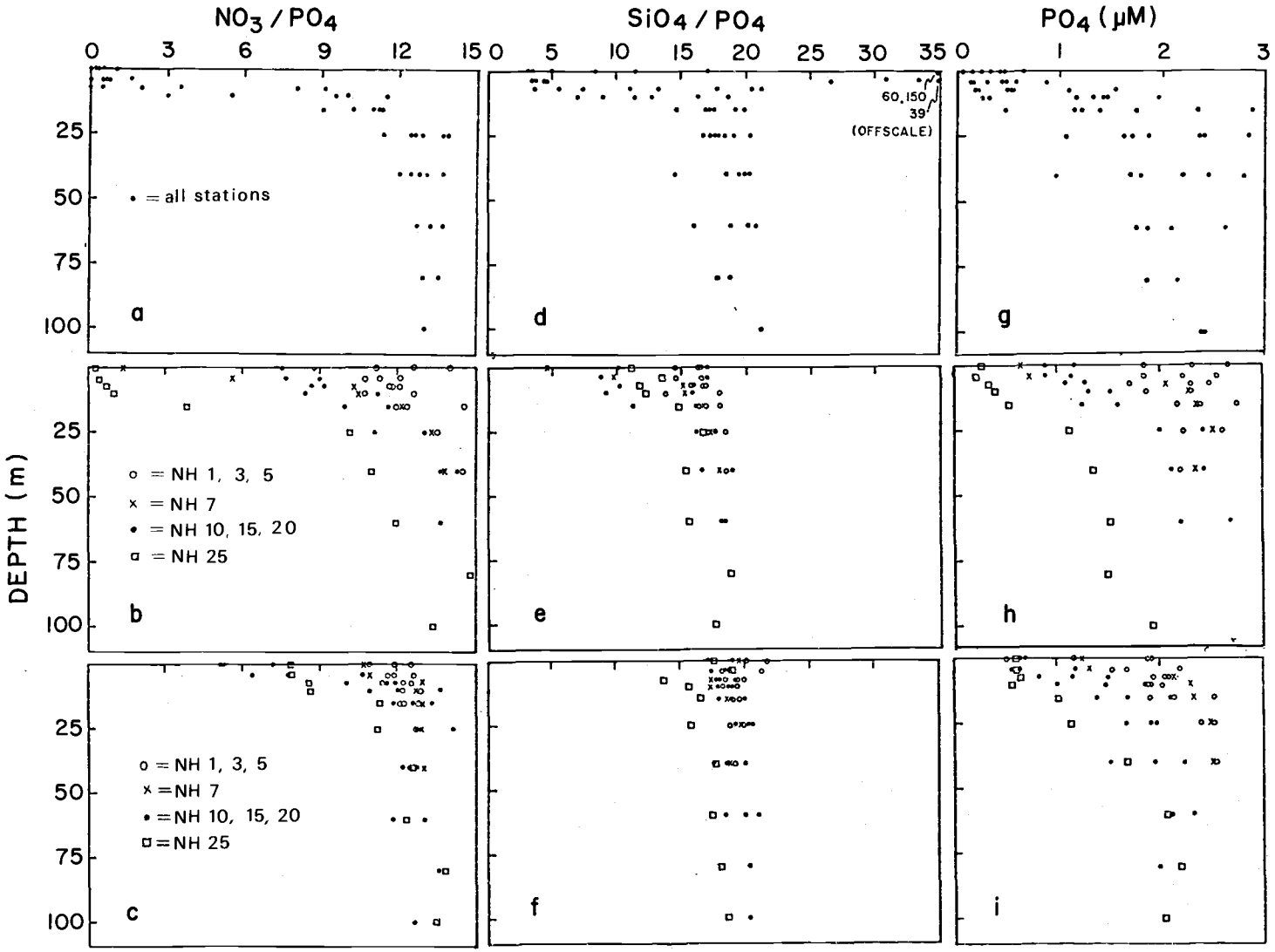

Figure 22. N:P, Si:P and phosphate (μM) versus depth for 1NH (a, d, g), 2NH (b, e, h), and 3NH (c, f, i).

The depth of this gradient corresponds roughly to the average depth of the euphotic zone (as determined from secchi disc readings taken throughout the cruise).

The extremely high Si:P ratios offshore are the result of excess SiO_4 relative to PO_4 contributed by the Columbia River. These high ratios are found when the surface salinity is less than 31‰, further indication of the presence of river water. Further inshore, however, the Si:P ratios drop in the surface waters, with some intermediate values arising from a mixture of inshore and river water. The pattern with depth follows closely that seen in the N:P ratio. Ratios on the order of 3-5 are seen at the surface increasing to the 18-20 range below 15-25 m. The low surface Si:P ratio suggests a lack of SiO_4 because of a recent diatom bloom.

The second running of the NH line was taken after upwelling had recommenced. Notably, the inshore stations showed an increase in N:P and Si:P ratios at the surface of about 10-13, making them comparable to the averages in deep water on the previous line. Further offshore, the N:P ratio had increased somewhat, with surface N:P values at 2NH-25 little changed from before. The surface N:P (and Si:P) ratio at 2NH-7 was anomalously low. (This patch of anomalous water has been noted before in other sections.) A somewhat different trend is also observed for N:P and PO_4 in the deep waters at 2NH-25, both N:P and PO_4 showing lower values compared to other values at

comparable depths. Si:P ratios for this station are slightly, though not so noticeably, lower than the other stations. No explanation is readily apparent for this discrepancy. The similarity between the PO_4 and N:P diagrams is evident for this section. Surface PO_4 concentrations have risen at the inshore stations by slightly more than 2 μM, while those offshore remained relatively low. Both the N:P and PO_4 diagrams for this section seem to show less vertical structure than the Si:P plot. The high Si:P ratios observed offshore during 1NH have been replaced by values slightly lower than typical deeper-water values.

There is a marked contrast in vertical structure between the Si:P and PO_4 plots for the final NH-line. All values for Si:P, with the exception of some at 3NH-25, lie clustered about 18-20, regardless of depth. The PO_4-depth relation, however, has begun to assume a character more nearly like that in the first section. Stations inshore of NH-20 show a decrease of ~ 0.5 μM PO_4 compared to the 2NH section; 3NH-25 showed an increase of approximately the same amount. N:P ratios have begun to cluster around 12-13, with some lower values in the surface waters offshore of NH-10. Note that the surface N:P ratio at NH-25 has increased by about 8, while the surface waters at NH-10, -15, and -20 showed a slight decrease. This trend follows that observed in the PO_4 distribution. It is interesting that while the N:P ratio remained relatively low in the offshore

surface waters, the corresponding Si:P ratio continued to be constant with depth. This may indicate that, relative to phosphate, nitrate begins to be depleted from the surface waters before silicate, or is being regenerated more slowly, though this could be the result of mixing with river water. As was seen in the first section, a reduced N:P ratio corresponded to a low Si:P ratio, except where the water was influenced by the Columbia River.

Combining both N:P and Si:P ratios can be useful in determining, to some extent, the origin and "photosynthetic age" of surface waters during upwelling. For this series on the Newport line, Table 5 may be constructed (the numerical limits given below should only be regarded as approximate values).

Table 5. Interpretation of surface nutrient ratios in the Oregon upwelling regime.

Sfc N:P	Sfc Si:P	Comment
Low (0-2)	Low (3-5)	Recent or active photosynthesis, not recently affected by upwelling
High (10-13)	Med (16-20)	Active upwelling area; photosynthesis not yet started
Low (0-2)	Med-high (15->30)	Columbia River water influence; active photosynthesis
Med (5-10)	Med (16-20)	Mixing of older and freshly upwelled water; beginning of photosynthetic activity

Oxygen, Temperature, and Salinity

The existence of a locally formed water mass, characterized by a temperature inversion, has been postulated by Mooers et al. (1972) and is mentioned elsewhere in this study. This offshore-moving water, which sinks near the base of the permanent pycnocline, shows evidence of having been at the surface. It was heated by insolation (and possibly further altered by mixing across the surface frontal zone) but its salinity remains relatively high. Although the sinking water is warmer than surrounding waters, it is more dense than the surface waters further offshore, and it sinks below the surface. Its density is such that the water column remains stable. Further evidence that this water has had recent surface contact might also be found in the dissolved gas distribution. As noted earlier, the water which upwells near the coast is highly undersaturated with respect to atmospheric oxygen. Upon reaching the surface, photosynthesis (possibly) and contact or exchange with the atmosphere will raise the level of dissolved oxygen. One might expect, then, an oxygen anomaly corresponding to the temperature inversion. (This anomaly is discussed also in the context of preformed nutrient changes in the section dealing with that topic.)

Figure 23 presents the T-S and O_2-S relationships for the Newport line on each of the three different occupations. There is a striking correspondence between the shapes of the temperature and

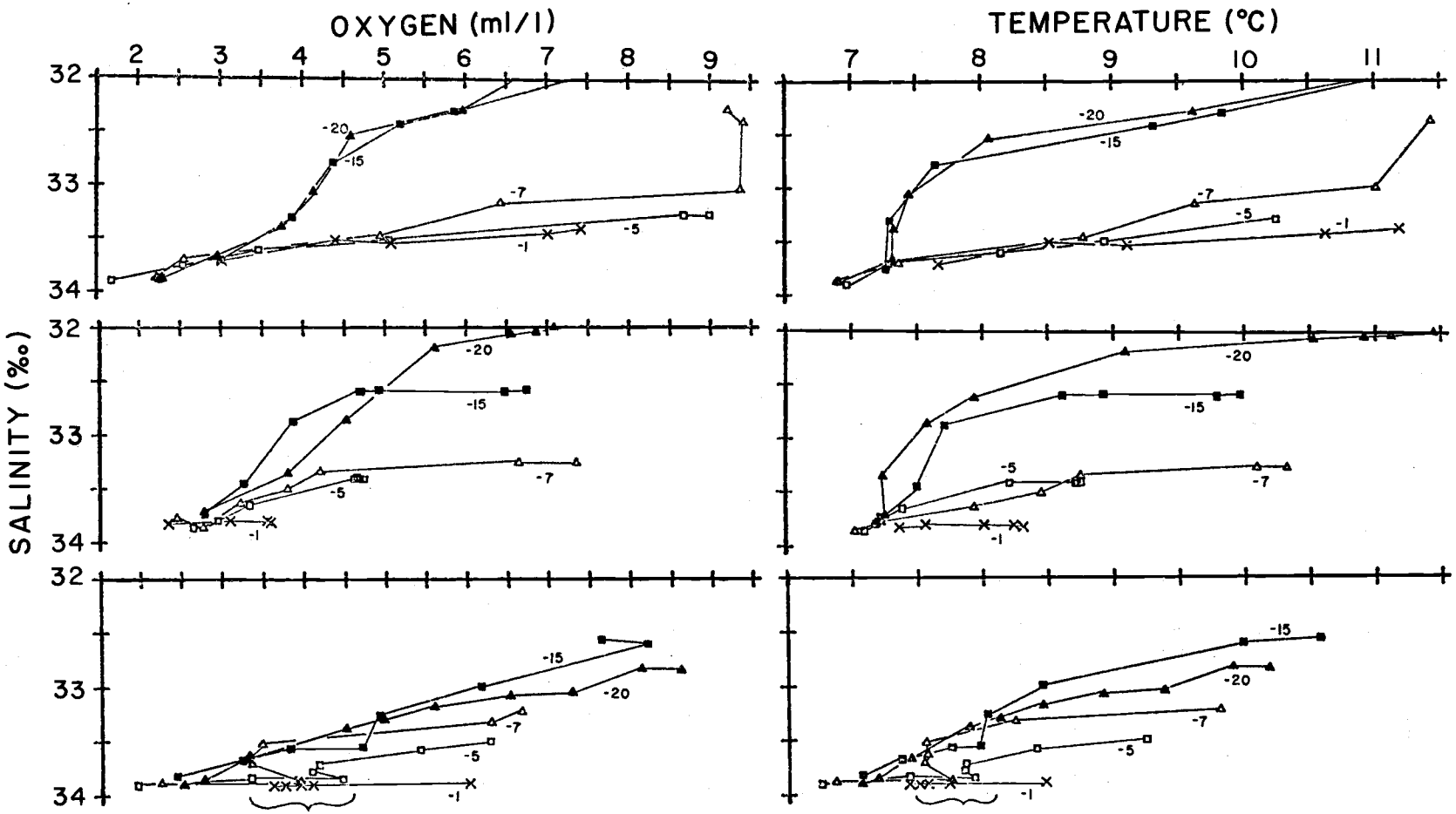

Figure 23. Oxygen-salinity and temperature-salinity relationships for 1NH (a, b), 2NH (c, d), and 3NH (e, f). Note inversions indicated by brackets.

oxygen curves. Notice especially that there are oxygen inversions corresponding to the temperature inversions at 3NH-5 and -7 (indicated by brackets). These O_2 inversions arise from a combination of photosynthesis and air-sea exchange (see AOU-P.PO_4 section). The T-S character of the inversions seen here suggests recent formation; diffusion has not yet broadened the inversion (see Figure 16 for an expanded diagram). The main contributing factor to the inshore temperature distribution has been warming; only very slight salinity changes are observed. This is contrasted to a temperature inversion seen at 2NH-25 (see Figure 7). The latter shows a much broader salinity range, and it is more typical of the ones presented in Mooers et al. (1972). This inversion was not seen during 1NH and is not seen in 3NH. It is possible that this inversion "drifted in" from further north. (Temperature inversions were seen also during the OR and DB lines, though only one was observed south of the NH line. This was at A-5, and it also showed an oxygen inversion. The BC-line, in between A and NH, showed no inversions.) The broader temperature inversion at 2NH-25 showed no corresponding oxygen inversion.

There are several reasons why the dissolved oxygen concentration is not, and should not be expected to be, a permanent tag on the temperature-inversion water. Besides the physical factors which alter the dissolved oxygen concentration (diffusion, mixing, solubility

effects), there are biological factors which will also change the oxygen concentration (respiration, photosynthesis). The dissolved oxygen concentration in the offshore moving water mass will be affected primarily by in situ respiration as it sinks below the euphotic zone. Also oxidation of matter sinking from the surface (as opposed to that matter entrained in the water mass) will change the O_2 concentration in this parcel of water. Because of the fairly high gradient of oxygen in the upper 100 or so meters, i.e., in the region of the temperature-inversion water, maxima and minima may not be seen directly as such, but rather as relative deviations from a "normal" (i.e., unperturbed) vertical distribution. Two examples of this (from the DB line) are shown in Figure 24. The difficulty, of course, is determining a "normal" type distribution. It seems clear, though, that the coincidence of oxygen and temperature inversions does indicate recent surface contact. Mechanisms outlined above will change the characteristics of the temperature and oxygen concentration as the sinking parcel of water moves offshore.

In the course of looking at oxygen-temperature relationships on the Newport line, an apparent shift in the slope of O_2 versus T was noticed for the post-upwelling period covered by 3NH compared to the previous NH lines. Figure 25 shows the O_2-T relationship for all stations on the Newport line. After eliminating oxygen values above 100% saturation, a linear regression on each was performed. The

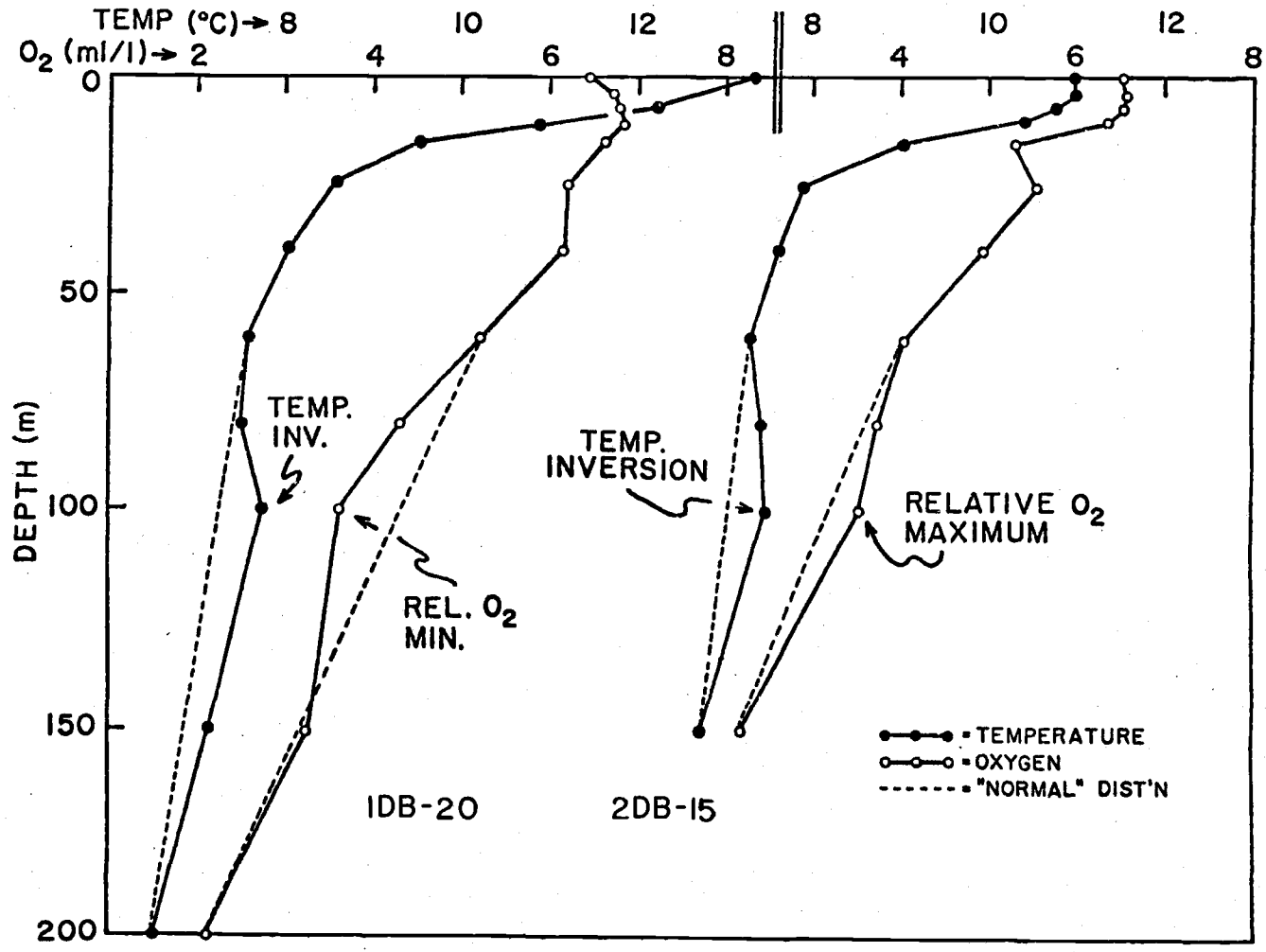

Figure 24. Depth profiles of oxygen and temperature from the DB line. See text for explanation.

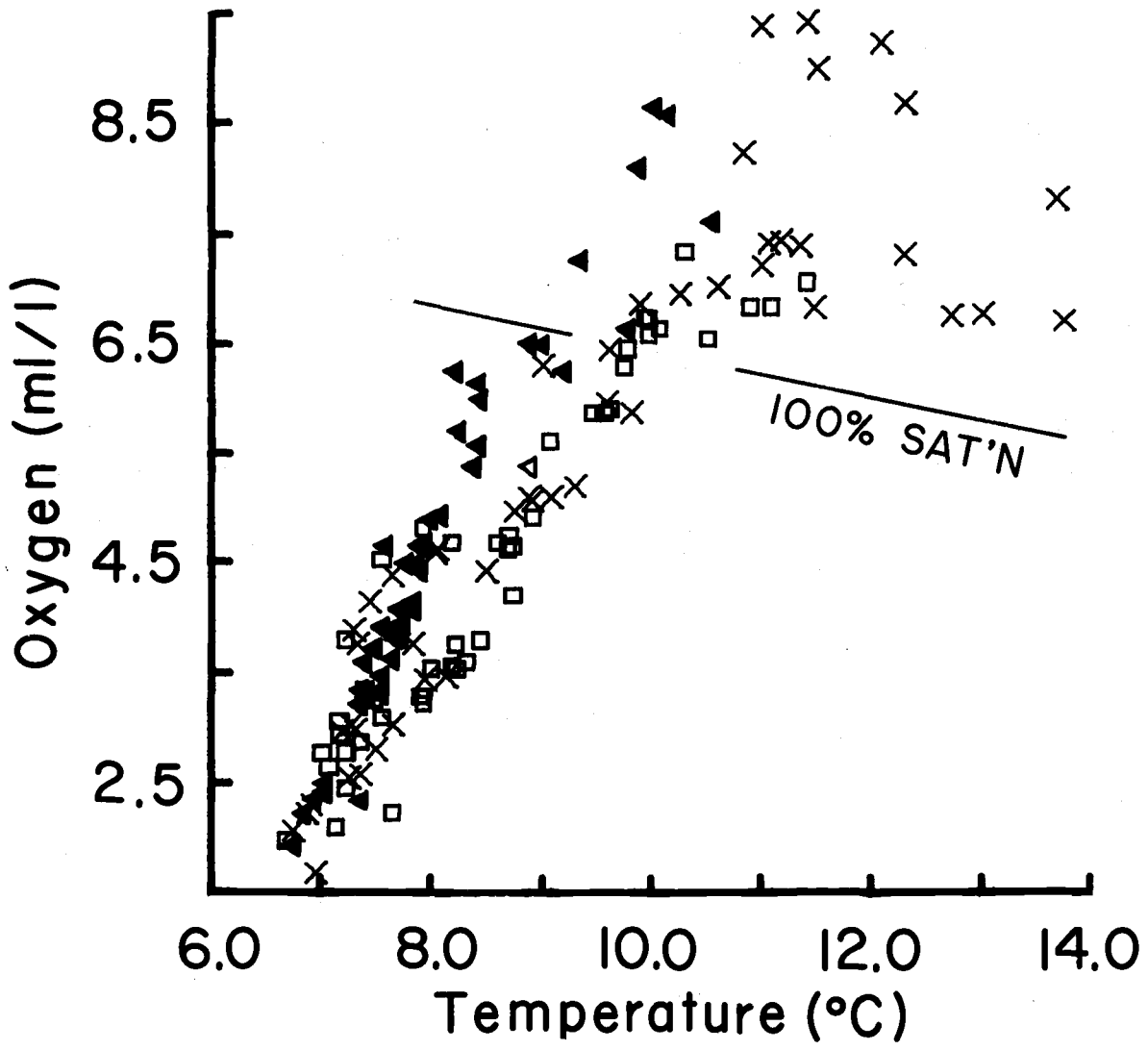

Figure 25. Oxygen-temperature relationships for all stations on the Newport hydrographic line. X = 1NH, □ = 2NH, ▲ = 3NH. The 100% saturation line was computed with a salinity of 33‰.

results are:

for 1NH, O_2 = -6.7(±1.7) + 1.33(±.21)T°C; (R^2 = .846) (5)

for 2NH, O_2 = -6.1(±1.5) + 1.25(±.19)T°C; (R^2 = .780) (6)

for 3NH, O_2 = -10.6(±1.4) + 1.90(±.18)T°C; (R^2 = .894) (7)

A significant increase in slope is seen for 3NH. 1NH and 2NH, below 100% saturation, show essentially the same relationship between O_2 and T.

Figure 25 shows that the main difference between 1NH and 2NH is the disappearance of a large portion of supersaturated water. The change in slope primarily indicates a generally cooler water section for the NH line. The difference in intercept is a function of the change in slope (see Equations 5, 6, 7). This is because the relationship must pivot about the source water value (if the source water remains the same). In this case the source water appears to be characterized by approximately 7.0°C, 2.5 ml/l O_2, and 33.9‰ S. This is typical of water found in the range of 150-200 m at approximately 50 km offshore. Reappearance of supersaturated waters is seen at the surface of 3NH-10-25, though stations inshore of these remain undersaturated.

Below 100% saturation, the correlation is best for the 3NH line. This might indicate a system more strongly dominated by physical factors. When biological processes occur, less of a correlation

might be expected. It is possible, too, that during inter-, or not-so-strong, upwelling periods the flow regime is less structured. This might also affect the correlation of the oxygen-temperature relationship.

The region above 100% saturation is also interesting. As can be seen in Figure 25 there is a significant break in the O_2-T relationship during 1NH. It is tempting to conjecture that this might give some indication of oxygen escape from the sea surface. The magnitude of the break, however, suggests the influence of the Columbia River plume. Reviewing the vertical sections of O_2 and T (see 1NH section in Figures 7 and 10) one sees that the maximum oxygen concentration occurred slightly shoreward of the area influenced by Columbia River water. As mentioned earlier (p. 64), the entire surface layer from the coast to NH-25 was supersaturated with oxygen. Furthermore, Columbia River water will be relatively warmer than adjacent waters (Cissell, 1969). Thus, it will have the effect of shifting the values on an O_2-T field to the right. The fact that local patchiness in the oxygen distribution placed the oxygen maximum away from the temperature maximum (i.e., in river water) moves points on an O_2-T field slightly down. It is this combination which had the greatest influence on producing the observed relationship.

This is not to say that oxygen transfer from the sea to the

atmosphere cannot qualitatively produce a similar pattern. Indeed, it must, considering the conditions off the Oregon coast. Generally, temperature decreases fairly monotonically with depth off Oregon. Plotting the O_2-T relationship for a region with a subsurface O_2 maximum would necessarily yield a pattern similar to that seen in Figure 25. In fact, several values from 1NH and 3NH show this effect. The main difference is the exaggerating influence of Columbia River water. Thus, much of the correlation in the near surface layers is the result of the chance location of phytoplankton blooms relative to the Columbia River plume and to the coincidence of the general oxygen and temperature decrease off the Oregon coast. Several possibilities, then, become apparent for the O_2-T relationship off the coast of Oregon. Some of these are indicated schematically in Figure 26. Three cases are presented in this figure. The first case shows a general oxygen-temperature relationship in the absence of Columbia River influence. This case yields a fairly linear correlation, with a slight break due to oxygen loss to the atmosphere. The oxygen maximum for this case is fairly near the surface; both the temperature and oxygen difference between the subsurface maximum and the surface is relatively small. The second case indicates presence of Columbia River plume water offshore of the oxygen maximum. The relatively higher temperature and lower oxygen of plume water mask any effect due to possible oxygen loss.

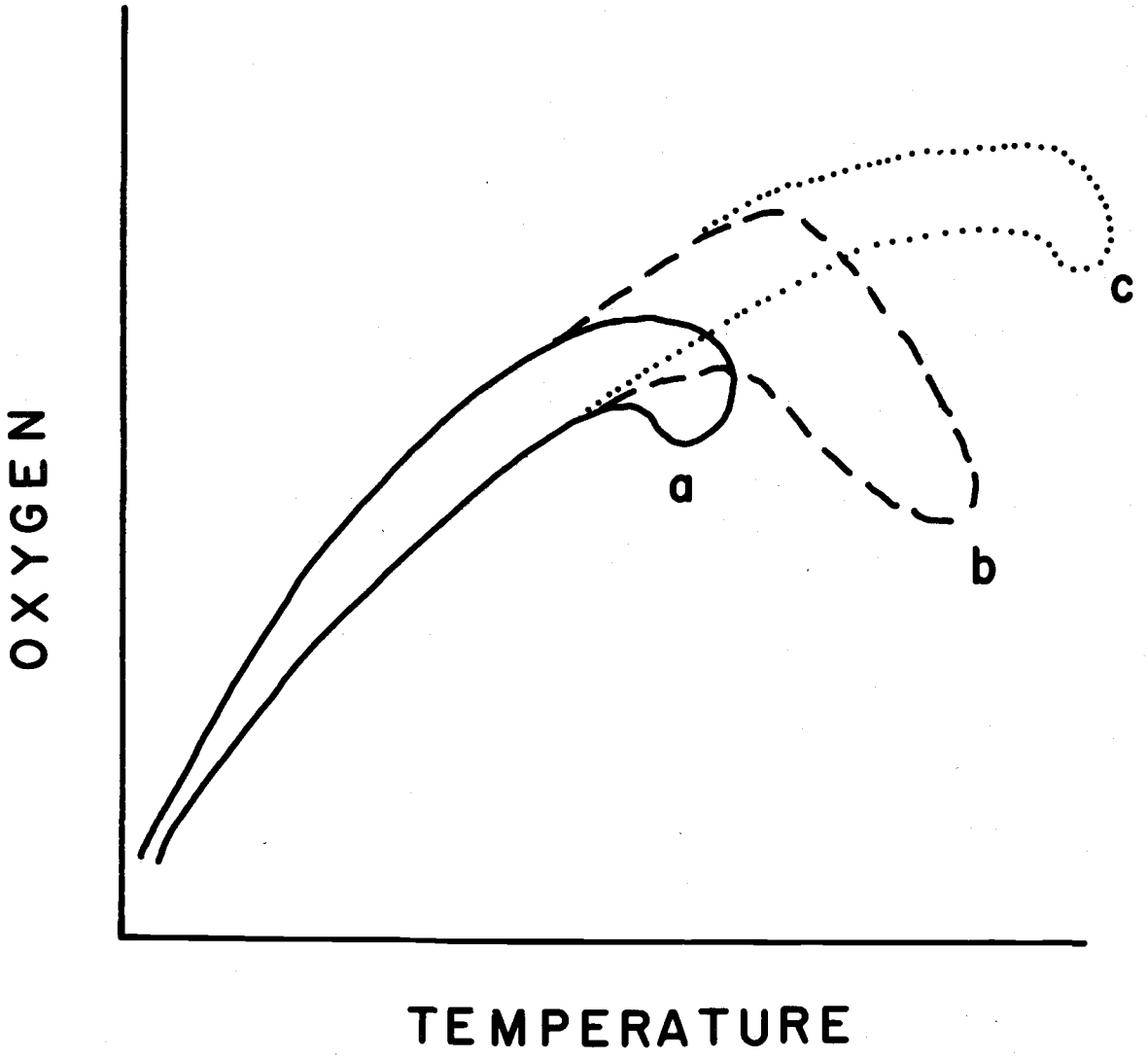

Figure 26. Schematic oxygen-temperature relationship. a) indicates loss of oxygen to the atmosphere, but the absence of Columbia River plume influence. b) indicates the presence of Columbia River plume waters, but the maximum in oxygen concentration is inshore of the plume. c) indicates maximum oxygen concentration within plume area, and some loss to the atmosphere.

The second case corresponds to the situation observed during 1NH. The last case, in which the oxygen maximum is located in the Columbia River plume, is purely hypothetical. Nutrient supply to plume water is inhibited because of the large density gradient associated with the plume. Thus, one does not find a great deal of phytoplankton activity within the plume area. It is presented as merely an illustrative example to be compared to the other two cases.

CHAPTER FIVE

SUMMARY AND CONCLUSIONS

The events described in this work show the rapid changes which can take place during upwelling off the Oregon coast. Work currently being done (CUE, 1972) indicates that the time scale and magnitude of the observed changes are not atypical of events during upwelling.

The factors affecting upwelling are by no means constant. Future work will have to consider changes in chemical parameters over several time scales - from hours to months - in order to better understand the upwelling system. The primarily advective nature of the changes observed on Y7006A made conclusions somewhat simpler to obtain.

These conclusions may be summarized as follows:

1. Large changes in chemical distributions can occur within a time scale of several days. The greatest fluctuations were observed within 10 to 15 km of the coast. Changes occurring on a smaller time scale (< 1 day) can also be significant. For cruise Y7006A changes in the chemical distributions resulted primarily from advective transport, biological activity, and interaction with Columbia River water. The roles of mixing and diffusion were not assessed.

2. The velocity structure calculated from the salinity distribution on the Newport line shows a pattern common for upwelling: offshore velocities ranging from 2-18 cm/sec in the surface layers; onshore velocities are in the range of 1-2 cm/sec. The velocity distribution calculated for the 21st to 28th of June suggests a tongue of offshore moving water sinking below the permanent pycnocline.

3. Transport calculated from the salinity distribution compares well with that computed from wind data. For the 276 hour time interval, both methods show that approximately 8×10^9 g/cm were transported onshore. This corresponds to an onshore transport of nutrients of 1.7, 22, and 38 moles/day/cm of PO_4, NO_3, and SiO_4, respectively.

4. The possibility of large gradients in chemical properties at the surface allows these variables to be quite useful in identification of freshly upwelling waters. This confirms observations by others. Also, because of the different response times of water motion and biological activity, a combination of biological and hydrographic parameters can be used to identify various stages of upwelling.

5. A comparison of PO_4 concentrations on surfaces of constant sigma-t indicated a nutrient source low in the water column of the inshore stations. Remineralization of organic detritus in the shelf sediments is likely a large contributor to this source.

6. The flux of oxygen is from the atmosphere to the sea in

water which has recently upwelled. This is expected because the water arriving at the surface is undersaturated with respect to atmospheric oxygen. This effect is also reflected in the preformed nutrient values. Biological activity will also increase the oxygen content of the surface waters.

7. The combination of NO_3: PO_4 and SiO_4: PO_4 ratios can indicate, to some extent, the origin and "photosynthetic age" of upwelled water. These ratios also indicate an abundance of phosphate relative to silicate and nitrate (compared to normal assimilation ratios).

8. Temperature inversions were found to coincide with oxygen inversions at inshore stations after upwelling had continued for approximately 12 days. These inversions suggest recent contact with the atmosphere and tend to support the conceptual model of upwelling presented by Mooers et al. (1972). That not all temperature inversions contained oxygen inversions can be explained by in situ oxidation of detritus both entrained in and falling through the water mass, and by mixing and diffusion.

BIBLIOGRAPHY

Alvarez-Borrego, S. 1973. Oxygen-carbon dioxide-nutrients relationships in the Northeastern Pacific Ocean and Southeastern Bering Sea. Doctoral dissertation. Corvallis, Oregon State University. 171 numb. leaves.

Arthur, R. S. 1965. On the calculation of vertical motion in eastern boundary currents from determinations of horizontal motion. Journal of Geophysical Research 70: 2799-2804.

Atlas, E. L., S. W. Hager, L. I. Gordon and P. K. Park. 1971. A practical manual for use of the Technicon AutoAnalyzer® in seawater nutrient analyses; revised. 49 numb. leaves. (Oregon State University, Dept. of Oceanography, Technical report 215, Reference no. 71-22).

Anderson, D. H. and R. J. Robinson. 1946. Rapid electrometric determination of the alkalinity of sea water using a glass electrode. Industrial and Engineering Chemistry, Analytical Edition 18: 767-773.

Ball, D. S. 1970. Seasonal distribution of nutrients off the coast of Oregon, 1968. Master's thesis. Corvallis, Oregon State University. 71 numb. leaves.

Brown, N. L. and B. V. Hamon. 1961. An inductive salinometer. Deep-Sea Research 8: 65-75.

Calvert, S. E. and N. B. Price. 1971. Upwelling and nutrient regeneration in the the Benguela Current, October, 1968. Deep-Sea Research 18: 505-523.

Cissell, M. C. 1969. Chemical features of the Columbia River plume off Oregon. Master's thesis. Corvallis, Oregon State University. 45 numb. leaves.

Collins, C. A. 1964. Structure and kinematics of the permanent oceanic front off the Oregon coast. Master's thesis. Corvallis, Oregon State University. 53 numb. leaves.

Collins, C. A., C. N. K. Mooers, M. R. Stevenson, R. L. Smith and J. G. Pattullo. 1968. Direct current measurements in the frontal zone of a coastal upwelling region. Journal of the Oceanographical Society of Japan 24: 295-306.

CUE. 1972. CUE (Coastal Upwelling Experiment) NOTES. Nos. 1-11. School of Oceanography, Corvallis, Oregon State University. Unpublished manuscripts.

Gilbert, W. 1972. Computer Programmer, Oregon State University, School of Oceanography. Personal communication. Corvallis, Oregon.

Gordon, L. I. 1973. A study of carbon dioxide partial pressures in surface waters of the Pacific Ocean. Doctoral dissertation, Corvallis, Oregon State University. 216 numb. leaves.

Grill, E. V. and F. A. Richards. 1964. Nutrient regeneration from phytoplankton decomposition in seawater. Journal of Marine Research 22: 51-69.

Hager, S. W. 1969. Processes determining silicate concentrations in the northeastern Pacific Ocean. Master's thesis. Corvallis, Oregon State University. 58 numb. leaves.

Hurlburt, H. E. and J. D. Thompson. 1972. Coastal upwelling on a β-plane. Unpublished manuscript (Submitted to Journal of Physical Oceanography).

Jones, P. G. W. 1971. The southern Benguela Current region in February, 1966: Part I. Chemical observations with particular reference to upwelling. Deep-Sea Research 18: 193-208.

Jones, P. G. W. 1972. The variability of oceanographic observations off the coast of north-west Africa. Deep-Sea Research 19: 405-431.

Kantz, K. W. 1973. Chemistry and hydrography of Oregon coastal waters and the Willamette and Columbia Rivers: March and June, 1971. Master's thesis. Corvallis, Oregon State University. 70 numb. leaves.

Kolthoff, I. M., E. B. Sandell, E. J. Meehan and S. Bruckenstein. 1969. Quantitative chemical analysis. 4th ed. New York, Macmillan. 1199 p. See p. 973-975.

Mooers, C. N. K. 1970. The interaction of an internal tide with the frontal zone of a coastal upwelling region. Doctoral dissertation. Corvallis, Oregon State University. 480 numb. leaves.

Mooers, C. N. K., C. A. Collins and R. L. Smith. 1972. The dynamic structure of the frontal zone in the coastal upwelling region off Oregon. Unpublished manuscript (Submitted to Journal of Physical Oceanography).

Oregon State University, Department of Statistics. 1971. Statistical Instruction Programming System (SIPS). Preliminary User's Guide. Corvallis. 25 p. Unpublished manuscript.

Pak, H., G. F. Beardsley, Jr. and R. L. Smith. 1970. An optical and hydrographic study of a temperature inversion off Oregon during upwelling. Journal of Geophysical Research 75: 629-636.

Park, K., J. G. Pattullo and B. Wyatt. 1962. Chemical properties as indicators of upwelling along the Oregon coast. Limnology and Oceanography 7: 435-437.

Park, K. 1965. Gas chromatographic determination of dissolved oxygen, nitrogen, and total carbon dioxide in sea water. Journal of the Oceanographical Society of Japan 21: 28-29.

Park, K. 1967. Nutrient regeneration and preformed nutrients off Oregon. Limnology and Oceanography 12: 353-357.

Park, K. 1968. Alkalinity and pH off the coast of Oregon. Deep-Sea Research 15: 171-183.

Pattullo, J. and W. Denner. 1965. Processes affecting seawater characteristics along the Oregon coast. Limnology and Oceanography 10: 443-450.

Pillsbury, R. D. 1972. A description of hydrography, winds, and currents during the upwelling season near Newport, Oregon. Doctoral dissertation. Corvallis, Oregon State University. 163 numb. leaves.

Poole, H. H. and W. R. G. Atkins. 1929. Photo-electric measurements of submarine illumination throughout the year. Journal of the Marine Biological Association, United Kingdom 16: 297-324. (Cited in: Sverdrup, H. U., W. Johnson, and R. H. Fleming. 1942. The oceans. New York, Prentice-Hall, Inc. 1087 p.)

Pytkowicz, R. M. 1964. Oxygen exchange rates off the Oregon coast. Deep-Sea Research 11: 381-389.

Pytkowicz, R. M. 1968. Water masses and their properties at 160° W in the Southern Ocean. Journal of the Oceanographical Society of Japan 24: 21-31.

Pytkowicz, R. M. 1971. On the apparent oxygen utilization and the preformed phosphate in the oceans. Limnology and Oceanography 16: 39-42.

Pytkowicz, R. M. and D. R. Kester. 1966. Oxygen and phosphate as indicators for the deep intermediate waters in the northeast Pacific Ocean. Deep-Sea Research 13: 373-379.

Redfield, A. C. 1942. The processes determining the concentration of oxygen, phosphate and other organic derivatives within the depths of the Atlantic Ocean. Papers in Physical Oceanography and Meteorology 9. 22 p.

Redfield, A. C. 1948. The exchange of oxygen across the sea surface. Journal of Marine Research 7: 347-361.

Redfield, A. C., B. H. Ketchum and F. A. Richards. 1963. The influence of organisms on the composition of seawater. In: The sea. Vol. 2. ed. by M. N. Hill, New York, John Wiley & Sons. p. 26-77.

Smith, R. L., J. G. Pattullo and R. K. Lane. 1966. An investigation of the early stage of upwelling along the Oregon coast. Journal of Geophysical Research 71: 1135-1140.

Smith, R. L. 1968. Upwelling. Oceanography and Marine Biology Annual Reviews 6: 11-46.

Stefánsson, U. and F. A. Richards. 1963. Processes contributing to the nutrient distributions off the Columbia River and Strait of Juan de Fuca. Limnology and Oceanography 8: 394-410.

Stefánsson, U. and F. A. Richards. 1964. Distributions of dissolved oxygen, density, and nutrients off the Washington and Oregon coasts. Deep-Sea Research 11: 355-380.

Strickland, J. D. H. and T. R. Parsons. 1968. A practical handbook of seawater analysis. Fisheries Research Board of Canada, Ottawa. Bulletin 167. 311 p.

Wyatt, B., R. Tomlinson, W. Gilbert, L. Gordon and D. Barstow. 1971. Hydrographic data from Oregon waters, 1970. 134 numb. leaves. (Oregon State University, Dept. of Oceanography. Data report 49, Reference no. 71-23, on Office of Naval Research Contract N00014-67-A-0369-0007 Project NR 083-102 and NSF Grant GA 12113)

Wyatt, B., R. Tomlinson, W. Gilbert, L. Gordon and D. Barstow. 1972. Hydrographic data from Oregon waters, 1971. 77 numb. leaves. (Oregon State University, Dept. of Oceanography. Data report 53, Reference no. 72-14, on Office of Naval Research Contract N00014-67-A-0369-0007 Project NR 083-102 and NSF Grant GA 12113)